Reinstatement of cortical outcome representations during higher-order learning

Lennart Luettgau[1,2,3*], Emanuele Porcu[4], Claus Tempelmann[5], Gerhard Jocham[1,2]

[1]Biological Psychology of Decision Making, Institute of Experimental Psychology, Heinrich Heine University, Universitätsstrasse 1, 40225 Düsseldorf, Germany

[2]Center for Behavioral Brain Sciences, Otto-von-Guericke University, Universitätsplatz 2, 39106 Magdeburg, Germany

[3]Max Planck University College London Centre for Computational Psychiatry and Ageing Research, Russell Square House 10-12 Russell Square, WC1B 5EH London, UK

[4]Department of Biological Psychology, Otto-von-Guericke University, Universitätsplatz 2, 39106 Magdeburg, Germany

[5]Department of Neurology, Otto-von-Guericke University, Leipziger Strasse 44, 39120 Magdeburg

*Correspondence to: luettgau@hhu.de

Abstract

Naturalistic learning scenarios are characterized by infrequent experience of external feedback to guide behavior. Higher-order learning mechanisms like second-order conditioning (SOC) may allow stimuli that were never experienced together with reinforcement to acquire motivational value. Despite its explanatory potential for real-world learning, surprisingly little is known about the neural mechanism underlying such associative transfer of value in SOC. Here, we used multivariate cross-session, cross-modality searchlight classification on functional magnetic resonance imaging data obtained from humans during SOC. We show that visual first-order conditioned stimuli (CS) reinstate cortical patterns representing previously paired gustatory outcomes in the lateral orbitofrontal cortex (OFC). During SOC, this OFC region showed increased functional covariation with amygdala, where neural pattern similarity between second-order CS and outcomes increased from early to late stages of SOC. Our data suggest a mechanism by which motivational value is conferred to stimuli that were never paired with reinforcement.

Significance Statement

Despite its prevalence in naturalistic learning scenarios and its importance for adaptive behavior, how stimuli that have themselves never been directly paired with reinforcement acquire motivational value remains unclear. Here, we use a second-order conditioning paradigm and multivariate functional neuroimaging analyses in humans to show that first-order conditioned stimuli reinstate representations of previously associated outcomes in the lateral orbitofrontal cortex. Interactions between orbitofrontal cortex and amygdala may support associative linking of second-order conditioned stimuli and outcomes, allowing for associative transfer of value in higher-order learning. These findings present a neural mechanism for transfer of motivational value to stimuli that were never directly paired with reinforcement.

Introduction

Learning in naturalistic settings is characterized by infrequent direct encounters with rewarding or punishing stimuli (Gewirtz and Davis, 2000). Hence, several stimuli or actions often need to be chained together, such that one stimulus serves as a proxy for another stimulus that might eventually predict reward (Gewirtz and Davis, 2000). Exploiting such statistical regularities would allow agents to learn about the value of stimuli or actions that were never directly followed by reinforcement and support instrumental behavior in the absence of reinforcement or in new contexts. Second-order conditioning (SOC) is an example of higher-order learning that allows such associative transfer to stimuli that have never been directly paired with reinforcement (Pavlov, 1927; Rizley and Rescorla, 1972). In SOC, a first-order conditioned stimulus (CS_1) is first paired with a motivationally salient event or stimulus (unconditioned stimulus, US). By virtue of this pairing, the CS_1 is capable of evoking conditioned responses (CR, e.g. salivating, as in the presence of food), enabling it to function as conditioned reinforcer (Sharpe et al., 2017). Subsequently, another previously neutral conditioned stimulus (CS_2) is paired with the CS_1. Thereby, CS_2 acquires incentive properties and is, like CS_1, now able to elicit a CR. Despite its relevance for real-life learning phenomena (Gewirtz and Davis, 2000; Parkes and Westbrook, 2011) and decades of behavioral investigations (Rizley and Rescorla, 1972; Barnet et al., 1991; Gewirtz and Davis, 2000; Parkes and Westbrook, 2011), surprisingly little is known about the neural mechanism underlying associative transfer of motivational value in SOC (Parkes and Westbrook, 2011).

Building on models of memory reinstatement (Tonegawa et al., 2018), we hypothesized that during SOC, presentation of the CS_1 would trigger reinstatement of the neural pattern representing the US with which it had previously been paired during first-order conditioning (FOC). This would allow linkage of CS_2 and US representations by associative plasticity. Both amygdala (Hatfield et al., 1996; Gewirtz and Davis, 1997, 2000; Setlow et al., 2002; Parkes and Westbrook, 2011) and hippocampus (Gilboa et al., 2014), as well as orbitofrontal cortex (OFC) and ventral striatum (Mcdannald et al., 2013) have consistently been shown as the key structures involved in second-order learning and conditioned reinforcement (Hatfield et al.,

1996; Gewirtz and Davis, 1997, 2000; Setlow et al., 2002; Parkes and Westbrook, 2011; Gilboa et al., 2014). Our analyses therefore focused on these regions.

To test our predictions, we combine a SOC paradigm and choice preference tests with cross-session (Stokes et al., 2009), cross-modality searchlight (Kriegeskorte et al., 2006) classification of functional magnetic resonance imaging (fMRI) data in healthy human participants. Participants first established Pavlovian associations between visual CS_1 and appetitively or aversively valued gustatory US. During SOC, participants were exposed to associations between visual CS_2 and previously learned CS_1. In a subsequent preference test phase, participants were more likely to select directly (CS_1) and indirectly (CS_2) appetitively paired stimuli over aversively paired stimuli. These behavioral associative transfer learning effects were accompanied by CS_1-related reinstatement of the neural patterns representing US in the lateral OFC and increased functional coupling between lateral OFC, amygdala/anterior hippocampus, and medial OFC during SOC. Furthermore, representations of second-order CS in the amygdala became more similar to US representations from early to late phases of second-order conditioning, indicating the acquisition of an association between CS_2 and US patterns.

Materials and Methods

Experimental design and statistical analyses

Participants were recruited from the local student community of the Otto-von-Guericke University Magdeburg, Germany by public advertisements and via online announcements. Only participants indicating no history of psychiatric or neurological disorder, no regular intake of medication known to interact with the central nervous system and participants not reporting quinine intolerance were included. Participants in both samples had normal or corrected-to-normal vision and did not report experience with Japanese kanjis or Chinese characters. All participants provided informed written consent before participation and received monetary compensation for taking part in the study. The study was approved by the local ethics committee at the medical faculty of the Otto-von-Guericke University Magdeburg, Germany

(reference number: 101/15) and conducted in accordance with the Declaration of Helsinki. We assumed a medium effect size in a generic binomial test (effect size g = 0.25) for the main behavioral effects (choice probability > 0.50), for which a sample size of N = 23 would be necessary, given standard power ($1–\beta$ = 0.80) and a one-tailed alpha-error probability of 0.05.

We conducted two experimental studies. Since we used within-subject designs in both experiments and each participant experienced all conditions, effects of interest were tested within-subjects. There were no experimental groups and thus no randomization to experimental group was performed. 32 healthy adult volunteers (age: M = 24.16, SD = 3.61 years, 15 males) participated in the fMRI study. We recruited 32 participants due to the fact that we expected ~15% drop out in the fMRI sample (due to compromised data, artifacts, falling asleep etc.). 20 healthy adult volunteers (age: M = 23.40, SD = 3.07 years, 9 males), participated in the behavioral study. In the fMRI study, two participants were excluded from statistical analyses due to self-reports of having fallen asleep during the second-order conditioning scanning run. One additional participant had to be excluded due to a scanner malfunction and corruption of three of the five classifier training experiment scanning runs, thus leaving a total of N = 29 participants for final analyses.

In the fMRI study, volunteers participated in two sessions on two consecutive days (Figure 1A). The fMRI classifier training (see below) took place on the first day, and the learning experiment (next paragraph) was performed on the second day. In the behavioral study, participants attended one single session during which they performed the learning experiment.

Learning experiment – ratings

Participants received written instructions for the experiment and were instructed once again on the computer screen. All experiments were programmed in MATLAB 2012b (v8.0.0.783, MATLAB and Statistics Toolbox Release 2012b, The MathWorks, Inc., Natick, MA, USA), using Psychophysics Toolbox (Brainard, 1997) (version 3). Before and after the learning experiment, participants rated ten different round, greyscale fractal images (300 x 300 pixels) serving as first-order conditioned stimuli (CS_1), ten white Japanese kanjis (Tamaoka et al.,

2017) (250 x 250 pixels) serving as second-order conditioned stimuli (CS_2) and gustatory stimuli as unconditioned stimuli (US). We used quinine-HCl (0.2 mmol/l solved in purified water) as aversive US and either chocolate milk (Nesquik, Nestlé, Switzerland) or orange juice (Milde Orange, EDEKA, Germany) as appetitive US (only orange juice in the fMRI study). Each participant received the same kind and amount of US per trial during the experiment. Ratings of subjective value/liking were assessed with the number buttons on a German (QWERTZ) computer keyboard from 1 (not liked) to 9 (very much liked). In the fMRI sample, participants additionally rated gustatory stimuli regarding their subjective intensity levels from 1 (low intense) to 9 (very intense). Three fractals and kanjis rated closest to 5 (equivalent to "neutral") were selected for first- and second order conditioning and their order was randomized before being associated with the US in first-order conditioning or with the first-order CS_1 in second-order conditioning. To ensure motivational salience of the gustatory US, participants were instructed to abstain from food for 12 hours and on average reported having fasted for 13.28 (*SD* = 2.71) hours. Participants reported intermediate levels of hunger before the task on a paper-pencil visual analog scale (VAS), ranging from 0 ("not hungry") to 100 ("very hungry"), *M* = 58.38 (*SD* = 29.61).

Learning experiment – first-order conditioning

The first-order conditioning (FOC) phase of both the fMRI study and the behavioral study was performed outside of the scanner (Figure 1C). This was aimed at avoiding fatigue effects during the second-order conditioning phase, which was the phase of main interest to test our neural hypotheses. During FOC, participants were presented with CS^+_1 followed by the appetitive US^+, and CS^-_1 followed by the aversive US^-. CS_1 were presented for 2000 ms, followed by an inter-stimulus interval (1000 ms) marked by a fixation cross, and oral infusion of one US (1 ml bolus per trial). Each CS_1 was presented 50 times, amounting to 100 trials total. CS_1 were followed by a US with 80% probability (40 trials of each CS_1-US pair, 10 trials of CS_1-no US per CS). US were delivered by a MATLAB code-controlled custom-made gustometer consisting of two high pressure single syringe pumps (AL-1000HP, World Precision

Instruments, Saratoga, FL) operating 50 ml Luer lock syringes. Syringes were attached to Luer lock infusion lines (1,40 m length, 2 mm inner diameter) that participants held centrally in their mouths like drinking straws. In the fMRI study, infusion line position order (Q-O (*N* = 17) and O-Q (*N* = 15) for quinine (Q) and orange juice (O)), i.e. which US was delivered from the left or right infusion line, was counterbalanced across participants. In the fMRI study, the US bolus onset was preceded (500 ms) by a blue square that was presented for 2500 ms on the screen (Figure 1C). Participants were instructed to only swallow the US bolus upon offset of the blue square. Each trial was separated by an inter-trial-interval (ITI) marked by a grey screen. The ITI per trial was drawn from a discretized γ-distribution (shape = 6, scale = 1) truncated for an effective range of values between 3500 ms and 10,000 ms. Participants took self-paced breaks after each 10th trial during which they could drink water. Importantly, the instructions did not contain information about the underlying associative structure of the experiment, aiming at leaving participants unaware of the associative learning process. Instead, participants were instructed to perform a simple attentional control task, during which they should respond as quickly and as correctly as possible by pressing the "y" button upon seeing the CS_1 colored in red. Each CS_1 was colored red in 10 % of the trials (90 % of trials grayscale image) and color did not predict US contingency. Performance during the task was rewarded with a bonus of 1 € (if > 70 % correct answers). Participants performed very well in the attentional control task (overall probability of correct answers: *M* = .99, *SD* = .05). In the fMRI sample, both ratings and first-order conditioning were performed outside the MRI scanner.

Learning experiment – second-order conditioning

In the fMRI study, second-order conditioning (SOC) was performed inside the MRI scanner. For SOC, participants were presented with CS_2^+ followed by CS_1^+, CS_2^- followed by CS_1^- and CS_2^n followed by CS_1^n. CS_1^n had not been presented during first-order conditioning and thus was not paired with any US. The novel CS_2^n-CS_1^n pair served to control for attentional and novelty effects. In each trial (Figure 1D), a CS_2 (2000 ms) was followed by an inter-stimulus interval (500 ms) marked by a fixation cross, and a CS_1 (2000 ms). CS_2 were followed by a

CS_1 deterministically. Each trial was separated by an ITI marked by a grey screen. The ITI per trial was drawn from a discretized γ-distribution (shape = 7, scale = 1) truncated for an effective range of values between 4000 ms and 10,000 ms. Each CS_2-CS_1 pair was presented 50 times, amounting to 150 trials total. Again, instructions did not explicitly mention relational structures to be learned, but participants were instructed to perform a simple attentional control task. Participants were instructed to respond as quickly and as correctly as possible by pressing the "y" button (behavioral study) or with the right index finger on an MRI-compatible 4-button response box (fMRI study) upon seeing the CS_2 tilted by a 45° angle. Each CS_2 was tilted in 10 % of its presentations. Performance during the task was rewarded with a bonus of 1 € (if > 70 % correct answers). Participants performed very well in the attentional control task (overall probability of correct answers: *M* = .97, *SD* = .07).

Learning experiment – choice preference test

Following SOC, participants were presented with two separate test phases consisting of repeated binary choices (30 trials) between pairs of CS_1 and pairs of CS_2 to assess behavioral signatures of first- and second-order conditioning. Each choice between CS_1^+ and CS_1^-, and between CS_2^+ and CS_2^- was presented ten times (twelve times in the fMRI sample). We hypothesized preference for both CS_1^+ and CS_2^+ over CS_1^- and CS_2^-, respectively, as expressed by choice probabilities above indifference criterion (choice probability > 0.5). Decision trials were interleaved with choices between the novel CS_1^n or CS_2^n and lure stimuli (fractal or kanjis, respectively) that had only been seen during pre-task rating in pseudo-random order. These novel-to-lure comparison trials were intended to rule out response biases related to mere exposure to the stimuli experienced during conditioning. We reasoned that if choices were reflecting acquired and transferred value and could not only be attributed to mere exposure-dependent response biases, choice probability in trials involving novel-to-lure stimuli should not exceed the indifference criterion. Choice options were presented for 1500 ms on the right- and left-hand side of the screen. If participants did not respond within this time-window, a time-out message was displayed, and the respective trial was repeated at the end

of the choice preference test. Order (left/right) of choice options was counterbalanced. Participants selected choice options by pressing the “y” (left option) or “m” (right option) button (behavioral sample, left or right index finger on MR-compatible response box in the fMRI sample). Participants were instructed to select the CS they preferred/liked more. Importantly, participants were never presented with the US related to their chosen or unchosen CS.

Behavioral analyses

Data were analyzed using MATLAB 2019a (v9.6.0.1072779, The MathWorks, Inc., Natick, MA, USA) and RStudio (RStudioTeam, 2019) (version 3.6.3, RStudio Team, Boston, MA) using custom analysis scripts. Choice probabilities for each CS in the fMRI and behavioral study were jointly analyzed. Each binary decision in which the respective CS was present (1 = selection of the respective target CS, 0 = selection of the alternative CS) for CS_1^+ and CS_2^+ (versus CS_1^- and CS_2^-, respectively) and both first-order and second-order novel-to-lure comparison trials was included in the models. We used six single-trial Bayesian multilevel generalized linear models (Equations 1–6), representing different hypotheses about which processes might have generated the choice data using the R package rethinking (McElreath, 2020): 1) “Flat” model, modelling a single intercept parameter, 2) “Flat” model with CS-specific intercepts, 3) Sample-specific intercepts model, allowing separate intercepts for both samples (fMRI and behavioral study) 4) Sample-specific intercepts model with covarying CS-specific intercepts, 5) Varying intercepts model, allowing an individual intercept drawn from a population hyperprior distribution for each subject with covarying CS-specific intercepts and thereby accounting for inter-individual variability in choice probabilities and 6) Model combining individually varying intercepts and sample/group-specific intercepts with covarying CS-specific intercepts. The relative model fits indicate whether it is indeed necessary to model group differences between samples. We used Pareto-Smoothed Importance Sampling (PSIS) for model comparisons and to find evidence for the best-fitting model. Within the best-fitting model, we hypothesized above-chance level choice probability for both CS_1^+ and CS_2^+ at the group-level. For both first-order and second-order novel-to-lure comparison trials, we expected no

difference from chance level for these choices. We specified weakly informative prior and hyperprior probability distributions, used a binomial distribution as likelihood function (e.g. Equation 1) and used the function "ulam" (rethinking), which passes the model to RStan (Development Team, 2020). Using No-U-Turn (NUTS; a variant of Hamiltonian Monte Carlo) samplers in RStan and four independent Markov chains we drew 4 x 10000 samples from posterior probability distributions (4 x 5000 warmup samples). Quality and reliability of the sampling process were evaluated with the Gelman-Rubin convergence diagnostic measure ($\hat{R} \approx 1.00$) and by visually inspecting Markov chain convergence using trace- and rank-plots. For all models fitted we found $\hat{R} = 1.00$ for all parameters sampled from the posterior distribution. There were no divergent transitions between Markov chains for any of the models reported. For hypothesis testing, we specified a region of practical equivalence (ROPE), i.e. an interval of parameter values (choice probability = [.45; .55]) representing the null hypothesis. Specifically, we expected that the 89% highest posterior density interval (HPDI) around the parameter estimates would not overlap with the ROPE for choices of CS_1^+ and CS_2^+ (versus CS_1^- and CS_2^-, respectively), allowing to reject the null hypothesis. However, the ROPE would overlap with the 89%-HPDI around the parameter estimates for both first-order and second-order novel-to-lure comparison trials. Overlap between HPDIs and ROPEs was quantified using the R package bayestestR (Makowski et al., 2019).

$$\begin{aligned} CP &\sim \mathrm{Binomial}(1, \mathrm{p}) \\ logit(p) &= \alpha \\ \alpha &\sim \mathrm{Normal}(0, 1) \end{aligned} \tag{1}$$

where *CP* is the binomially distributed choice probability for all CS (CS_1^+, CS_2^+, CS_1^n or CS_2^n). *p* is the proportion of choices of CS.

$$
\begin{aligned}
&CP_i \sim \text{Binomial}(1, \text{p}) \\
&logit(p) = \mu_\alpha + x_{CS[i]} * \sigma_\alpha \\
&\text{x}_{CS[i]} \sim \text{Normal}(0, 1) \\
&\mu_\alpha \sim \text{Normal}(0, 1) \\
&\sigma_\alpha \sim \text{Half} - \text{Normal}(0, 0.1)
\end{aligned} \tag{2}
$$

where CP_i is the binomially distributed choice probability for each CS seperately (CS_1^+, CS_2^+, CS_1^n or CS_2^n). p is the proportion of CS choices. Note that the model is reparametrized to allow sampling from a standard normal posterior distribution.

$$
\begin{aligned}
&CP_j \sim \text{Binomial}(1, p_j) \\
&logit(p_j) = \mu_\alpha + x_{group[j]} * \sigma_\alpha \\
&\text{x}_{group[j]} \sim \text{Normal}(0, 1) \\
&\mu_\alpha \sim \text{Normal}(0, 1) \\
&\sigma_\alpha \sim \text{Half} - \text{Normal}(0, 0.5)
\end{aligned} \tag{3}
$$

where CP_j is the binomially distributed choice probability for the j-th group across all CS. p_j is the proportion of CS choices. Again, the model is reparametrized to allow sampling from a standard normal posterior distribution.

$$
\begin{aligned}
&CP_{j,i} \sim \text{Binomial}(1, p_j) \\
&logit(p_{j,i}) = \mu_{group[j]} + \mu_{CS[i]} + \alpha_{group[j],CS[i]} \\
&\begin{bmatrix} \alpha_{j,1} \\ \alpha_{j,2} \\ \alpha_{j,3} \\ \alpha_{j,4} \end{bmatrix} \sim \text{MVNormal}\left(\begin{bmatrix} 0 \\ 0 \\ 0 \\ 0 \end{bmatrix}, \mathbf{S} \right) \\
&\mathbf{S} = \begin{pmatrix} \sigma_{group} & 0 \\ 0 & \sigma_{CS} \end{pmatrix} \mathbf{R} \begin{pmatrix} \sigma_{group} & 0 \\ 0 & \sigma_{CS} \end{pmatrix} \\
&\mu_{group} \sim \text{Normal}(0, 1) \\
&\mu_{CS} \sim \text{Normal}(0, 1) \\
&\sigma_{\text{group}} \sim \text{Half} - \text{Normal}(0, 0.05) \\
&\sigma_{\text{CS}} \sim \text{Half} - \text{Normal}(0, 0.05) \\
&\mathbf{R} \sim \text{LKJcorr}(2)
\end{aligned}
\tag{4}
$$

where $CP_{j,j}$ is the binomially distributed choice probability for the j-th group, with CS-specific intercepts. $p_{j,i}$ is the proportion of CS choices.

$$
\begin{aligned}
&CP_i \sim \text{Binomial}(1, p_{j,i}) \\
&logit(p_{j,i}) = \mu_{CS[i]} + \alpha_{subject[j],CS[i]} \\
&\begin{bmatrix} \alpha_{j,1} \\ \alpha_{j,2} \\ \alpha_{j,3} \\ \alpha_{j,4} \end{bmatrix} \sim \text{MVNormal}\left(\begin{bmatrix} 0 \\ 0 \\ 0 \\ 0 \end{bmatrix}, \mathbf{S} \right) \\
&\mathbf{S} = \begin{pmatrix} \sigma_{subject} & 0 \\ 0 & \sigma_{CS} \end{pmatrix} \mathbf{R} \begin{pmatrix} \sigma_{subject} & 0 \\ 0 & \sigma_{CS} \end{pmatrix} \\
&\mu_{CS} \sim \text{Normal}(0, 1) \\
&\sigma_{subject} \sim \text{Half} - \text{Normal}(0, 0.5) \\
&\sigma_{\text{CS}} \sim \text{Half} - \text{Normal}(0, 0.5) \\
&\mathbf{R} \sim \text{LKJcorr}(2)
\end{aligned}
\tag{5}
$$

where CP_i is the binomially distributed choice probability for the i-th subject, covarying with CS-specific intercepts. p_i is the proportion of CS choices.

$$
\begin{aligned}
&CP_{i,j} \sim \text{Binomial}(1, p_{i,j}) \\
&logit(p_{i,j}) = \mu_{CS[i]} + \alpha_{subject[j],CS[i]} + \mu_{group[k]} \\
&\qquad + \gamma_{CS[i],group[k]} \\
&\begin{bmatrix} \alpha_{j,1} \\ \alpha_{j,2} \\ \alpha_{j,3} \\ \alpha_{j,4} \end{bmatrix} \sim \text{MVNormal}\left(\begin{bmatrix} 0 \\ 0 \\ 0 \\ 0 \end{bmatrix}, \mathbf{S}_{\boldsymbol{subject}} \right) \\
&\begin{bmatrix} \gamma_{i,1} \\ \gamma_{i,2} \end{bmatrix} \sim \text{MVNormal}\left(\begin{bmatrix} 0 \\ 0 \\ 0 \\ 0 \end{bmatrix}, \mathbf{S}_{\boldsymbol{CS}} \right) \\
&\mathbf{S}_{\boldsymbol{subject}} = \begin{pmatrix} \sigma_{subject} & 0 \\ 0 & \sigma_{CS} \end{pmatrix} \mathbf{R}_{\boldsymbol{subject}} \begin{pmatrix} \sigma_{subject} & 0 \\ 0 & \sigma_{CS} \end{pmatrix} \\
&\mathbf{S}_{\boldsymbol{CS}} = \begin{pmatrix} \sigma_{CS} & 0 \\ 0 & \sigma_{group} \end{pmatrix} \mathbf{R}_{\boldsymbol{CS}} \begin{pmatrix} \sigma_{CS} & 0 \\ 0 & \sigma_{group} \end{pmatrix} \qquad (6) \\
&\mu_{CS[i]} \sim \text{Normal}(0, 1) \\
&\mu_{group[k]} \sim \text{Normal}(0, 1) \\
&\sigma_{subject} \sim \text{Half} - \text{Normal}(0, 0.1) \\
&\sigma_{\text{CS}} \sim \text{Half} - \text{Normal}(0, 0.1) \\
&\sigma_{group} \sim \text{Half} - \text{Normal}(0, 0.1) \\
&\mathbf{R}_{\boldsymbol{subject}} \sim \text{LKJcorr}(2) \\
&\mathbf{R}_{\boldsymbol{CS}} \sim \text{LKJcorr}(2)
\end{aligned}
$$

where $CP_{i,j}$ is the binomially distributed choice probability, j-th subject and the k-th group covarying with CS-specific intercepts. $p_{i,j}$ is the proportion of CS choices.

fMRI – classifier training experiment

The classifier training experiment was always performed on day 1 of two consecutive testing days. This was done to acquire unbiased estimates of the neural patterns representing the two US for training of a multivariate classification algorithm (multivariate pattern analysis, MVPA), before any association of the US with first- or second order CS had been acquired. Participants received oral instructions for the classifier training experiment and were instructed once again on the projection screen in the MRI. Before and after the experiment, participants rated gustatory US (aversive: quinine-HCL 0.1 mmol/l solved in purified water and appetitive: orange juice) according to subjective value/liking and intensity via button presses with their right and left index and middle fingers on a MRI-compatible 4-button response box. Ratings ranged from 1 (not liked/not intense) to 4 (very much liked/very intense) and were indicated by e.g. pressing the left middle finger corresponding to rating 1 or pressing the right index finger corresponding to rating 3. As on day 2, participants were instructed to abstain from food for 12 hours and on average reported to have fasted for 13.59 (*SD* = 2.18) hours. Participants reported intermediate levels of hunger before the experiment on a paper-pencil VAS, *M* = 48.50 (*SD* = 31.28). In each of the five total runs of the classifier training experiment, each US was administered twenty times (40 trials per run, 200 trials in total). Per trial, one US (1 ml bolus per trial) was delivered by a MATLAB code-controlled custom-made gustometer and Luer lock infusion lines (8.30 m length, 2 mm inner diameter). Participants held infusion lines centrally in their mouths like drinking straws. Additionally, infusion lines were fixed at absorbent materials attached to throat, chin and cheeks. The US bolus onset was preceded (500 ms) by a blue square that was presented in total for 4000 ms on the screen. Participants were instructed to only swallow the US bolus upon offset of the blue square. Each trial was separated by an ITI marked by a grey screen. The ITI was drawn from a uniform distribution with 5 discrete steps (range: 3000 – 7000 ms). Both US were presented in a pseudo-random order, thus reducing the influence of potentially confounding low-level features of the schedule (e.g. number of same/different US repetitions, different ITI lengths following each US). During each run of the classifier training experiment, participants performed a 0-back style attentional control task.

After a pseudo-random 20% of trials, participants were presented with probe trials in which they were asked to indicate which US they had received last ("pleasant" (US^+) or "unpleasant" (US^-)) via button presses with their right and left index fingers on an MRI-compatible response box. Correct responses were rewarded with 0.05 € and incorrect responses or time-out trials (without a response by the participant within 2500 ms after onset of the probe trial) resulted in a 0.05 € penalty which would be summed up as a bonus upon completion of the experiment. On average, participants earned a bonus of 1.86 € (*SD* = .11) during the classifier training experiment. Performance during the 0-back attentional control task was generally high (overall probability of correct answers, excluding time-out trials: *M* = .93, *SD* = .05).

fMRI – acquisition

During SOC, one run, and during the classifier training experiment, five runs of fMRI were acquired on a 3 Tesla Siemens PRISMA MR-system (Siemens, Erlangen, Germany), using a 64-channel head coil. Blood oxygenation level dependent (BOLD) signals were acquired using a multi-band accelerated T2*-weighted echo-planar imaging (EPI) sequence (multi-band acceleration factor 2, repetition time (TR) = 2000 ms, echo time (TE) = 30 ms, flip angle = 80°, field of view (FoV) = 220 mm, voxel size = 2.2 × 2.2 × 2.2 mm, no gap). Per volume, 66 slices covering the whole brain, tilted by approximately 15° in z-direction relative to the anterior–posterior commissure plane were acquired in interleaved order. The first 5 volumes of the functional imaging time series were automatically discarded to allow for T1 saturation. To ensure close spatial alignment of the slices acquired during both sessions, the AutoAlign technique provided by the vendor was applied. At the end of both testing days, a B_0 magnitude and phase map was acquired to estimate field maps for B_0 field unwarping during preprocessing (TR = 660 ms, TE 1 = 4.92 ms, TE 2 = 7.38 ms, flip angle = 60°, FoV = 220 mm). Additionally, before task-based fMRI on both days, a high-resolution three-dimensional T1-weighted anatomical scan (TR = 2500 ms, TE = 2.82 ms, FoV = 256 mm, flip angle = 7°, voxel size = 1 × 1 × 1 mm, 192 slices) covering the whole brain was obtained using a magnetization-prepared rapid acquisition gradient echo (MPRAGE) sequence. This scan was

used as anatomical reference to the EPI data during the registration procedure. For all cross-session classification analyses, SOC EPI data was referenced to orientation of the classifier training experiment.

fMRI – data preprocessing

All fMRI preprocessing steps were performed using tools from the Functional Magnetic Resonance Imaging of the Brain (FMRIB) Software Library (FSL, v5.0 and v6.0, Jenkinson et al., 2012). Preprocessing for each run of both classifier training task and SOC task included motion correction using rigid-body registration to the central volume of the functional time series (Jenkinson et al., 2002), correction for geometric distortions using the field maps and an n-dimensional phase-unwrapping algorithm (B_0 unwarping, Jenkinson, 2003), slice timing correction using Hanning windowed sinc interpolation and high-pass filtering using a Gaussian-weighted lines filter of 1/100 Hz. EPI images were registered to the high-resolution structural image using affine linear registration (boundary-based registration) and then to standard (MNI) space using linear (12 degrees of freedom) and nonlinear registration (Andersson et al., 2007a, 2007b). Functional data was not spatially smoothed. We applied a conservative independent components analysis (ICA) to identify and remove obvious artefacts. Independent components were manually classified as signal or noise based on published guidelines (Griffanti et al., 2017), and noise components were removed from the functional time series.

fMRI – searchlight classification analyses

We hypothesized that, during SOC, first-order CS would reinstate the neural pattern of the US with which they had previously been paired during FOC. We therefore expected that a multivariate classification algorithm trained on neural patterns evoked by the US (during the classifier training task) would be able to correctly predict the class of a paired CS_1 during SOC. Hence, we used a cross-session (Stokes et al., 2009), cross-modality searchlight (Kriegeskorte et al., 2006) classification approach to identify brain regions in which the CS class during SOC

could be predicted based on training the classifier during the classifier training experiment on day 1. General linear models (GLMs) were fitted into pre-whitened data space to account for local autocorrelations (Woolrich et al., 2001). For the searchlight classification analyses, the individual level (first level) GLM design matrix per run and participant of the classifier training experiment included four box-car regressors in total. Two regressors coded for onsets and durations of both US (each modelled as single events of 4000 ms duration) and two regressors coded onsets and durations of left and right button presses (delta stick functions on the recorded time of response button presses) and the six volume-to-volume motion parameters from motion correction during preprocessing were entered to account for residual head motion. The SOC run per participant included five box-car regressors in total. Three regressors coding for onsets and durations of all combinations of CS_2-CS_1 (CS_2^+/CS_1^+, CS_2^-/CS_1^-, CS_2^n/CS_1^n) trials (each modelled as single events of 4500 ms duration, due to the 100 % contingency of CS-CS pairs), one regressor coding onsets and durations of right button presses (delta stick functions on the recorded time of response button presses), one regressor coding onset and duration of the within-run pause (45 sec), and the six volume-to-volume motion parameters from motion correction during preprocessing were entered. Please note that for the SOC analyses, the CS_2-CS_1 presentations were modeled as single events. The close temporal succession of the two stimuli with a fixed inter-stimulus interval was chosen to obtain robust conditioning effects. This makes it difficult to obtain estimates of neural activity that can be unambiguously attributed to either the first- or second-order stimulus. Therefore, for this analysis (but see below for neural pattern similarity analyses) we chose to model them as single events. Please note however that this analysis is not aimed at separating out effects specific to either CS_1 or CS_2. Instead, we aim to detect reinstatement of US representations. If such reinstated US representations can be detected, they indeed can only be faithfully attributed to the CS_1, as the CS_2 had no association with the US.

Additionally, we performed an exploratory multivariate searchlight classification to distinguish between the spatial activation patterns (*t* maps) of US^+ versus US^- across the whole brain during the classifier training experiment. The aim of this analysis was to present an

overview over the whole-brain patterns allowing classification of the US. This analysis resulted in one whole-brain map of classification accuracies per participant. The classification analysis was performed using a 5-fold cross-validation scheme, iteratively training the classification algorithm on the difference between US^+ versus US^- on 4 (out of 5 runs) labeled training data sets and then assessing the out-of-sample predictive accuracy of the classifier on the remaining, left-out data set (1 out of 5 runs).

Regressors were convolved with a hemodynamic response function (γ-function, mean lag = 6 s, SD = 3 s). Each first level GLM included two or three (for classifier training experiment or SOC, respectively) contrasts to estimate individual per run *t*-statistic maps for each US or each CS_2-CS_1 pair (for classifier training experiment or SOC, respectively). For SOC, the activation pattern of CS_2^n/CS_1^n was subtracted from CS_2^+/CS_1^+ and CS_2^-/CS_1^- activation patterns. This was intended to account for general activation expected to result from visually presented CS and the visually presented swallowing cue coinciding with US presentation, which could have confounded classification accuracies.

All classification-based analyses were conducted in subject native (fMRI) space. Per-participant *t*-statistic maps were subjected to linear support vector machine (C-SVM, cost parameter C = 1) classification using the MATLAB-based multivariate pattern analysis toolbox CoSMoMVPA (Oosterhof et al., 2016). For cross-session, cross-modality classification, a classifier was trained on the spatial activation patterns of US^+ versus US^- (obtained from classifier training) and tested on the patterns of CS_2^+/CS_1^+ versus CS_2^-/CS_1^- during SOC within 3-mm searchlight spheres across the whole brain. For the exploratory multivariate searchlight classification between US^+ versus US^- patterns, we similarly used a 3-mm searchlight sphere across the whole brain. Each searchlight sphere classification accuracy was mapped to the center voxel of the sphere, resulting in one whole-brain map of classification accuracies per participant. Additionally, in cross-session, cross-modality classification we repeated this procedure 100 times per participant with randomly permuted class labels in the training data set (US^+ versus US^-) to create chance level maps. Before group level statistics, the normalization parameters obtained from preprocessing were applied to both whole-brain

classification accuracy maps and chance level maps for normalization to MNI space. The resulting normalized whole-brain maps were spatially smoothed with a Gaussian kernel (5 mm full-width half-maximum).

For cross-session, cross-modality classification, we used small-volume correction (P_{SVC}) to assess significance of clusters with above-chance level (0.5) classification accuracy. To correct for multiple comparisons, we used a meta-analysis-based explicit mask for functional activations related to the term “taste” in the Neurosynth data base (Yarkoni et al., 2011) (www.neurosynth.org), thresholded at $z > 7$. This value was chosen such that only meta-analytic clusters of activation, but not single voxels, survived thresholding. The Neurosynth-based mask encompassed, aside from the lateral OFC, functional activation clusters in bilateral anterior insula. In addition, we evaluated an anatomically and functionally defined region-of-interest (ROI) for the lateral orbitofrontal cortex (lOFC), our a priori ROI. This region has been implicated in higher-order gustatory processing, such as motivational aspects and discrimination of taste (Small et al., 1999; Kobayashi et al., 2004; Miranda, 2012), but also representation and adaptive changes of stimulus-outcome associations (Klein-Flügge et al., 2013; Boorman et al., 2016; Jocham et al., 2016; Luettgau et al., 2020). We thus reasoned that this brain region would be a well-suited candidate for associative coupling between visual conditioned stimuli and gustatory outcomes and the proposed associative transfer learning. We used two different approaches for lOFC ROI definition: 1) an independent anatomical mask of the lateral OFC (Harvard-Oxford Atlas) and 2) an independent functional ROI from a gustatory mapping study by Benz and colleagues (K. Benz, personal communication, 12/2019). This approach aimed at reducing inferential limitations related to arbitrary ROI definition.

Within the meta-analysis-based mask and the ROIs, we computed group-level random-effect cluster-statistics corrected for multiple comparisons in small volumes as implemented in CoSMoMVPA(Oosterhof et al., 2016). In brief, for 50,000 iterations, we randomly selected one chance level map per participant, calculated a group level z-statistic map for the respective permutation and finally compared the resulting cluster sizes drawn from this empirical null

distribution (50,000 samples) to the clusters in the "real" classification accuracy map (Stelzer et al., 2013). Since classifications accuracies below chance level are generally limited in interpretability, we considered clusters significant if $P_{SVC} < .05$ (one-tailed). Please note that due to the exploratory nature and illustrative purpose of the exploratory multivariate searchlight classification between US^+ versus US^- patterns, no multiple comparisons correction using random-effects cluster-statistics was performed in this analysis.

Additionally, we split participants into a high- or low-bias group, depending on their preference for the CS_2^+ (vs. CS_2^-) and compared classification accuracies within the small-volume corrected cluster. The cluster ROI was built in MNI space and the ROI was then back-projected into subject native space using inverse normalization parameters obtained during preprocessing to extract individual averaged classification accuracies from the ROI. Both groups' average extracted classification accuracies were separately tested against chance level (0.5) using one-sample Wilcoxon signed-rank tests. We report measures of effect size Cohen's $U3_1$ for one-sample Wilcoxon signed-rank tests (range: 0 – 1, .5 indicating no effect), calculated in the MATLAB-based Measures-of-Effect-Size-toolbox (Hentschke, 2020).

fMRI – functional covariation analyses

Our cross-session, cross-modality searchlight classification during SOC identified a cluster in the lOFC (see Results). We investigated functional covariation between lOFC and the rest of the brain during SOC using this lOFC cluster as a seed region in a psychophysiological interaction (PPI) analysis. For each participant, we set up two separate first-level PPI GLMs. The first PPI GLM was aimed at investigating general differences in BOLD signal covariation for both CS_2^+/CS_1^+ and CS_2^-/CS_1^- compared with CS_2^n/CS_1^n. It contained the following regressors: 1) the BOLD timeseries (preprocessed functional time series) of the lOFC seed as physiological regressor, 2) onsets and durations of CS_2^+/CS_1^+ and CS_2^-/CS_1^- pairs (magnitude coded as 1) and CS_2^n/CS_1^n (magnitude coded as –1) as psychological regressor and 3) the interaction between 1) and 2) as psychophysiological interaction regressor. The psychological regressor was convolved with a hemodynamic response function (γ-function, mean lag = 6 s,

SD = 3 s). The second PPI GLM aimed at investigating specific differences in covariation between CS_2^+/CS_1^+ and CS_2^-/CS_1^-. It contained the following regressors: 1) the BOLD timeseries (preprocessed functional time series) of the lOFC seed as physiological regressor, 2) onsets and durations of CS_2^+/CS_1^+ (magnitude coded as 1) and CS_2^-/CS_1^- pairs (magnitude coded as –1) as psychological regressor and 3) the interaction between 1) and 2) as psychophysiological interaction regressor. The psychological regressor was convolved with a hemodynamic response function (γ-function, mean lag = 6 s, *SD* = 3 s).

In addition to the main effects of the PPI regressors, we also investigated whether task-related functional covariation of lOFC with the rest of the brain was related to our behavioral index of second-order conditioning (choice probability of CS_2^+ vs. CS_2^-). For this, we entered the averaged second-order choice preference test data per subject as an additional regressor to the group level GLMs. In all analyses, contrast images from the first level were then taken to the group level and analyzed using mixed-effects analyses in FLAME1+2 (Beckmann et al., 2003). We used cluster-based correction with an activation threshold of $Z > 2.3$ and a cluster-extent threshold of $P < .05$ at whole-brain level to control for multiple comparisons.

fMRI – neural pattern similarity analyses

In addition to our classification-based approach, we investigated whether there was evidence for changes of neural pattern similarity across second-order conditioning. Specifically, we used a least-squares separate (LS-S) approach (Mumford et al., 2012) to deconvolve single-trial estimates of neural patterns representing CS_2 and CS_1. We then used these patterns to perform a template-based neural pattern similarity analysis (Wimber et al., 2015) (a variant of representational similarity analysis, RSA (Kriegeskorte et al., 2008)) between patterns of the two US during the classifier training experiment and all trial-specific CS_2/CS_1 patterns during the SOC run. We estimated two subject-specific GLMs per trial, one for both CS_1 and CS_2, containing the following regressors: 1) onset and duration of the respective trial to be estimated (each modelled as a single event of 2000 ms duration), 2) onsets and durations of the remaining CS_1 or CS_2 trials, respectively, 3) onsets and durations of all other CS_1 or CS_2 trials,

respectively. Additionally, one regressor coding onsets and durations of right button presses (delta stick functions on the recorded time of response button presses), one regressor coding onset and duration of the within-run pause (45 sec), and the six volume-to-volume motion parameters from motion correction during preprocessing were entered. For example, the GLM of the 25th trial of CS_1^+, contained one regressor (onset and duration) modelling this particular trial and one separate regressor (onsets and durations) for all remaining CS_1 trials but the 25th trial of CS_1^+ (149 other trials in total) and one separate regressor (onsets and durations) modelling all CS_2 trials. This procedure is assumed to allow for better deconvolution of events happening within close temporal proximity than standard least-squares-based approaches, which generally do not distinguish between overall and trial-specific error terms (Mumford et al., 2012; Abdulrahman and Henson, 2016). As we have detailed above (paragraph "fMRI – searchlight classification analyses"), the temporal relation between CS_1 and CS_2 makes it inherently difficulty to estimate separate activation patterns. While, for the searchlight classification, it is not important to separate out the individual CS contributions to the neural pattern, our analyses on changes in neural pattern similarity across the SOC phase do make different predictions for CS_1 and CS_2. We therefore used the deconvolution approach described above to mitigate the issue, but caution is warranted in interpreting these results.

Each first level GLM included one contrast to model activation related to the respective trial of interest versus baseline. The a priori ROIs of the bilateral amygdala were built in MNI space and back-projected into subject native space using inverse normalization parameters obtained during preprocessing. We used these individual ROIs for spatially constrained multivoxel pattern extraction from the respective contrast *t*-value maps. Similarity-based analyses were carried out using CoSMoMVPA (Oosterhof et al., 2016). We used 1−Pearson's product-moment correlation coefficient (1−*r*) as a measure of pairwise dissimilarity between trial-specific neural patterns and the US template. Within-subject pairwise neural dissimilarity was subtracted from 1 (to create a measure of neural pattern similarity) and Fisher-*Z* transformed to approximate normally distributed data more closely. CS_1^n-US^-/CS_2^n-US^- and CS_1^n-US^+/CS_2^n-US^+ early and late neural pattern similarity were subtracted from CS_1^--US^-

/CS_2^--US^- and CS_1^+-US^+/CS_2^+-US^+ early and late neural pattern similarity, respectively. We hypothesized that neural pattern similarity would show changes from early (first 25) to late (last 25) trials, as both CS_2^+ and CS_2^- should become more similar to their respective indirectly associated US, indicating associative learning transfer from CS_1 to CS_2. Contrarily, CS_1^+ and CS_1^- should, if anything, become less similar to the respectively paired US (e.g. due to extinction). Average change of early to late CS-US neural pattern similarity was analyzed at the group level with paired-samples t-tests. Due to the expected negative change for CS_1^+ and CS_1^- and the expected positive change for CS_2^+ and CS_2^- across trials, we used one-tailed tests accordingly.

Code Accessibility and Data Availability

Custom analysis code for the reported behavioral data analyses and the multivariate fMRI, behavioral data, extracted classification accuracies, neural pattern similarity matrices and thresholded, unthresholded statistical maps that support the findings of this study are available at GitHub (https://github.com/LLuettgau/higher_order_learning). There are restrictions to the availability of the neuroimaging raw data due to them containing information that could compromise research participant privacy/consent. Neuroimaging raw data are available upon reasonable request from the corresponding author (LL).

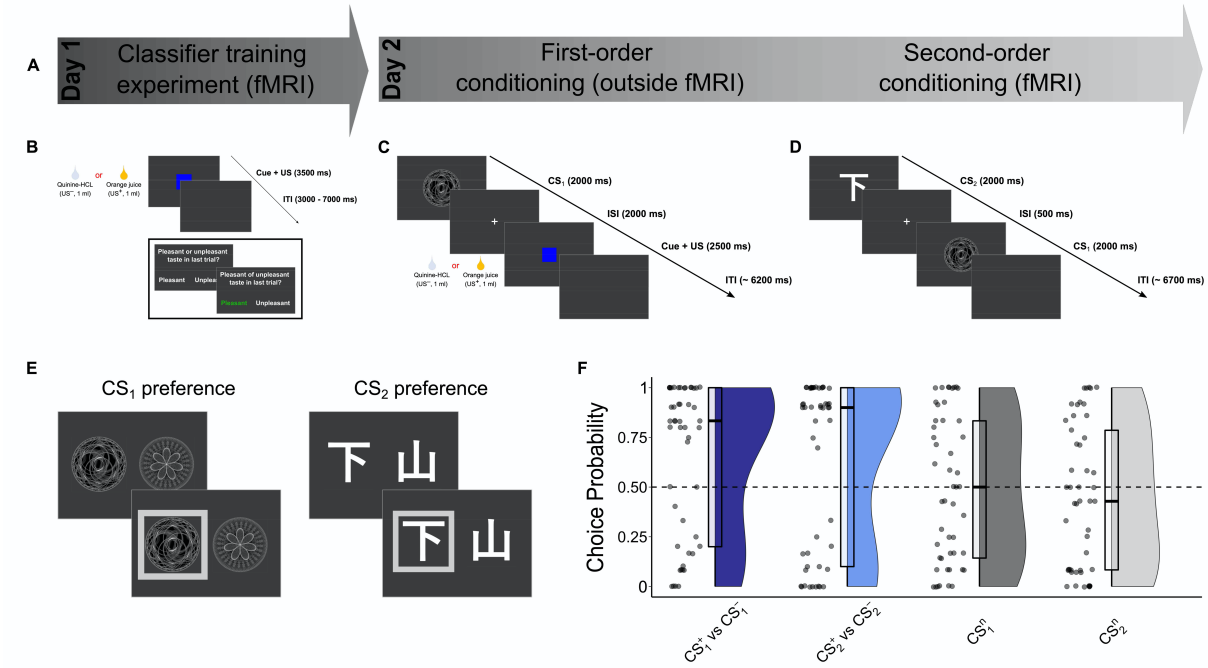

Figure 1. Experimental procedure, task schematic and behavioral results.

A) Experimental procedure: Participants in the fMRI study (*N* = 29) performed both day 1 and day 2 (B-E), participants in the behavioral study (*N* = 20) only performed the procedures of day 2 (C-E, outside fMRI). B) Classifier training experiment: After rating of subjective value and intensity of both gustatory US (orange juice and quinine), in a total of five runs each US was administered twenty times (40 trials per run, 200 trials in total). Per trial, one US (1 ml bolus per trial) was delivered. In the fMRI study, the US bolus onset was preceded by a blue square. Trials were separated by an inter-trial-interval (ITI) marked by a grey screen. Participants performed a 0-back-style attentional control task. In 20% pseudo-randomly selected trials, participants were presented with probe trials in which they were asked to indicate which US they had received last ("pleasant" (US^+) or "unpleasant" (US^-)). C) First-order conditioning (outside MRI): In each trial, a CS_1 was followed by an inter-stimulus interval marked by a fixation cross, and oral infusion of one US. Trials were separated by an ITI marked by a grey screen. CS_1 were followed by a US with 80% probability. D) Second-order conditioning: In each trial, a CS_2 was followed by an inter-stimulus interval marked by a fixation cross, and a CS_1. CS_2 were followed by a CS_1 fully deterministically. Each trial was separated by an ITI marked by a grey screen. E) Choice preference test: Following SOC, participants were presented with two separate test phases consisting of repeated binary choices between pairs of CS_1 (right) and pairs of CS_2 (left) to assess behavioral signatures of first- and second-order conditioning. F) Behavioral results (combined across fMRI and behavioral study, *N* = 49): Raincloud plots (Allen et al., 2019) showing density of choice probability. Box plot center lines represent (pre-averaged) sample medians and box bottom/top edges show $25^{th}/75^{th}$ percentile of the (pre-averaged) data, respectively.

Results

CS and US ratings

During the ratings prior to the learning experiment, the subjective values/liking of the three kanjis selected as CS_2 did not differ significantly from each other (main effect of stimulus: $F_{2,96}$ = 0.007, P = .993, η^2_p < .001, rmANOVA). However, there was a significant main effect of stimulus for the three fractals selected as CS_1 (main effect of stimulus: $F_{2,96}$ = 3.25, P = .043, η^2_p = .06, rmANOVA) that was driven by higher rating of CS_1^n than CS_1^- (t_{48} = 2.26, P = .028, paired-samples t-test). This difference most likely resulted from the selection process and the inherent rank-ordering of the CS according to subjective value ratings. However, there were no significant differences between CS_1^n and CS_1^+ (t_{48} = 1.68, P = .101, paired-samples t-test). Most importantly, no rating differences were observed between CS_1^- and CS_1^+ (t_{48} = 0.44, P = .659, paired-samples t-test). A rmANOVA evaluating changes in pre-post ratings indicated that none of the CS_1 was rated significantly different from the others across ratings (main effect of stimulus: $F_{2,96}$ = 3.09, P = .050, η^2_p = .06, rmANOVA). There was also no significant pre-post change in ratings across all CS_1 (main effect of time: $F_{1,48}$ = 2.02, P = .161, η^2_p = .04, rmANOVA). However, there was a significant CS x time interaction effect ($F_{2,96}$ = 3.36, P = .039, η^2_p = .07, rmANOVA), that was driven by more positive change of CS_1^+ ratings compared to CS_1^- (t_{48} = 2.06, P = .045, paired-samples t-test on pre-post differences) and CS_1^n (t_{48} = 2.52, P = .015, paired-samples t-test on pre-post differences), but no significant difference between CS_1^- and CS_1^n (t_{48} < .01, P > .999, paired-samples t-test on pre-post differences). Similarly, none of the CS_2 was rated significantly different from the others across ratings (main effect of stimulus: $F_{2,96}$ = .46, P = .606, η^2_p = .001, rmANOVA). There was significant pre-post change in ratings across all CS_2 (main effect of time: $F_{1,48}$ = 4.11, P = .048, η^2_p = .08, rmANOVA), resulting from slightly overall higher ratings after learning (mean difference: M = .29). However, here was no significant CS x time interaction effect for CS_2 ratings ($F_{2,96}$ = .89, P = .416, η^2_p = .02, rmANOVA).

Overall, US valence ratings did not differ from pre to post rating across both US (main effect of time (pre/post): $F_{1,48}$ = 0.34, P = .564, η^2_p = .01, rmANOVA), but the appetitive US^+

was – as expected – rated as significantly more pleasant than the aversive US$^-$ (main effect of stimulus: $F_{1,48}$ = 466.64, P < .001, η^2_p = .91, rmANOVA). There was also a significant interaction effect between stimulus and time, indicating that US$^+$ was rated as more pleasant and US$^-$ was rated as less pleasant from pre to post (interaction effect of stimulus x time: $F_{1,48}$ = 7.32 P = .009, η^2_p = .13, rmANOVA). Importantly, no subject rated US$^-$ as more pleasant than US$^+$ (pre or post). In the fMRI study, intensity ratings did not differ between US overall (main effect of stimulus: $F_{1,28}$ = 1.05, P = .315, η^2_p = .04, rmANOVA), but US were rated as significantly more intense at the post rating (main effect of time: $F_{1,28}$ = 4.89, P = .035, η^2_p = .15, rmANOVA). There was also a significant interaction effect between stimulus and time, indicating that US$^-$ intensity rating increased more strongly than US$^+$ from pre to post (interaction effect of stimulus x time: $F_{1,28}$ = 5.62, P = .025, η^2_p = .17, rmANOVA). The average temperature (°Celsius) of US$^+$ (M = 22.49, SD = 1.46) was significantly higher than temperature of US$^-$ (M = 22.37, SD = 1.52) before being loaded into the syringes (t_{27} = 2.22, P = .035, paired-samples t-test). However, we would argue that this minor difference in average temperatures (M = .12) is unlikely to be perceived by participants. Additionally, this difference does not meaningfully influence the observed results, since no neural activation was recorded during first-order conditioning and the multivariate classification analysis was trained on the data resulting from the fMRI classifier training experiment.

In the fMRI classifier training experiment, overall US valence ratings were higher in pre than in post rating (main effect of time (pre/post): $F_{1,28}$ = 11.67, P = .002, η^2_p = .29, rmANOVA), but the appetitive US$^+$ was, as intended, rated as significantly more pleasant than the aversive US$^-$ across ratings (main effect of stimulus: $F_{1,28}$ = 185.28, P < .001, η^2_p = .87, rmANOVA). There was no significant interaction effect between stimulus and time ($F_{1,28}$ = 0.28, P = .602, η^2_p = .01, rmANOVA). Importantly, no subject rated US$^-$ as more pleasant than US$^+$ (pre or post). Intensity ratings for US$^+$ were higher than for US$^-$ across ratings (main effect of stimulus: $F_{1,28}$ = 15.14, P < .001, η^2_p = .35, rmANOVA). There was no difference between US ratings from pre to post (main effect of time: $F_{1,28}$ = 0.02, P = .899, η^2_p < .001, rmANOVA). However, there was also a marginal interaction effect between stimulus and time, indicating that US$^-$

intensity rating increased while US^+ intensity rating decreased from pre to post (interaction effect of stimulus x time: $F_{1,28} = 3.93$, $P = .057$, $\eta^2_p = .12$, rmANOVA). Average temperature of US^+ ($M = 21.71$, $SD = 1.93$ °C) and US^- ($M = 21.68$, $SD = 1.95$) did not differ before being loaded into the syringes ($t_{27} = 0.71$, $P = .486$, paired-samples t-test).

Behavioral evidence for transfer of motivational value during second-order conditioning

Participants ($N = 49$, combined across two experiments) first established Pavlovian visuo-gustatory associations between a visual CS^+_1 and an appetitive gustatory US^+ (chocolate milk or orange juice), and between a visual CS^-_1 and an aversive gustatory US^- (quinine-HCl) during first-order conditioning (FOC, performed outside MRI, Fig. 1C). During SOC, participants were visually presented with CS_2^+ followed by CS_1^+, CS_2^- followed by CS_1^-, and a novel pairing of CS_2^n followed by CS_1^n (Fig. 1D). Since CS_1^n had not been presented during first-order conditioning, both CS_2^n and CS_1^n were considered neutral CS, serving as control stimuli for mere exposure effects and for correction of general visual activation effects in fMRI analyses (see Materials and Methods for details). Importantly, participants were not informed about the underlying associative structure of the tasks but were instructed to perform simple attentional control tasks. This was aimed at leaving participants unaware of the associative learning process. Post-experimental tests for explicit knowledge indeed revealed that participants were unaware of the (indirect) associations between CS_2 and US (Table 1). The number of participants that had indeed realized the indirect associations between CS_2 and US was significantly below the value that would be expected under a random guessing assumption (29%, $P = 0.004$, binomial test vs. 0.5). Participants could also not reliably indicate which CS_2 and which US had been indirectly linked in the experiment (mean correct responses: $M = 0.31$, $SD = 0.68$, maximum of 2 correct answers possible, Table 1). In a subsequent choice preference test (Fig. 1E), participants performed binary decisions between pairs of CS_1 and CS_2. Choice trials were interspersed with lure decisions between CS_1^n or CS_2^n and novel fractals or kanjis, respectively, that had only been seen during pre-task rating. We reasoned that choice probabilities should exceed the indifference criterion (choice probability > 0.5) if

Table 1. Explicit knowledge of CS-US associations

CS_1–US (*N* = yes)	CS_1–US (*Mean* + *SD*)	CS_2–US (*N* = yes)	CS_2–US (*Mean* + *SD*)
38 (78 %)	.98 (.95)	14 (29 %)	.31 (.68)

Note: Number (*N)* and percentage (in parentheses) of participants indicating explicit knowledge of CS–US associations between directly paired CS_1 and US (providing an answer to the question which CS_1 was associated with which US, regardless of being correct or incorrect) and indirectly paired CS_2 and US (responding "yes" to the question whether there was a relationship between CS_2 and US). These numbers of participants were significantly above (CS_1–US) and below (CS_2–US) the numbers expected under the assumption of random guessing, $P < .001$ and $P = .004$, respectively (Binomial test vs. 0.5). Additionally, we provide the mean (and standard deviation, *SD*) number of correct answers for CS–US associations between CS_1 and US, and CS_2 and US. Since participants were presented with two CS–US associations during conditioning, the maximum number of correct answers is 2 in both cases.

associative direct (CS_1) and associative transfer (CS_2) learning effects occurred. Additionally, we assumed that choice probability should not exceed the indifference criterion in trials involving novel-to-lure stimuli, if choice behavior was not exclusively driven by mere exposure or novelty-dependent response biases. Combined across the two experiments, participants showed a preference both for the appetitive first- and second order stimuli, CS_1^+ and CS_2^+, respectively, over the aversive CS_1^- and CS_2^- (Fig. 1F).

Among six candidate Bayesian multilevel generalized linear models (Methods), a model that combined individually varying intercepts for each participant with covarying CS-specific intercepts (Equation/Model 5) best captured the observed pattern of choice behavior (Pareto-Smoothed Importance Sampling (PSIS) values ($\pm$ standard error): Model 5 = 1788.6 ($\pm$53.13), Model 6 = 2034.8 ($\pm$33.53), Model 4 = 3173.2 ($\pm$18.37), Model 2 = 3184.5 ($\pm$15.64), Model 3 = 3236.6 ($\pm$8.34), Model 1 = 3239.1 ($\pm$8.12). This model had higher predictive accuracy than any other model considered and captured the choice behavior more accurately than the more complex model combining individually varying intercepts, sample/group-specific intercepts with covarying CS-specific intercepts (Equation/Model 6). This suggests that adding group/sample as a predictor does not meaningfully increase the predictive accuracy of the

model over and above what can be explained by individual intercepts combined with covarying CS-specific intercepts, to capture inter-individual variability in choice behavior. Within the varying intercepts model (Equation/Model 5), the highest posterior density intervals (HPDI) around the group-level intercept parameter (i.e. the mean posterior choice probability, μ_α= .71) for CS_1^+ versus CS_1^- [.61; .81] and for CS_2^+ versus CS_2^- (μ_α= .69) [.56; .81] did not overlap (0% overlap) with the defined ROPE (choice probability = [.45; .55]). Importantly, there was no evidence for both choice probabilities of CS_1^n (μ_α= .50) and CS_2^n (μ_α= .42) being different from chance level in novel-to-lure comparison choice trials (Fig. 1F, HPDIs: [.38; .62] and [.31; .53], 57.43% and 28.05% ROPE overlap, respectively). This indicates that our conditioning procedure reliably induced both direct associative (CS_1) and associative transfer learning effects (CS_2). The observed pattern of results rules out an explanation of CS_1^+ and CS_2^+ preference arising from mere-exposure or novelty. Together, these data indicate that our conditioning procedures induced both a preference of CS_1^+ over CS_1^-, and of CS_2^+ over CS_2^-.

First-order CS reinstate neural US patterns during second-order conditioning

After establishing behavioral evidence for associative transfer learning, we reasoned that a prerequisite for the observed learning effect would be reinstatement of the neural US pattern by the paired CS_1 to establish a direct associative link between CS_2 and US. Importantly, it should be noted that US reinstatement during SOC could only be faithfully attributed to the respective CS_1, but not to CS_2, since only CS_1 had been directly paired with the US, and CS_2 had not previously been experienced. To test for cortical reinstatement of neural patterns representing US during second-order conditioning, we used functional magnetic resonance imaging (fMRI) and a cross-session (Stokes et al., 2009), cross-modality searchlight (Kriegeskorte et al., 2006) classification approach (multivariate pattern analysis, MVPA). To obtain unbiased estimates of the neural patterns representing our gustatory US, without the confounding influence of associations to a learned first-order CS, we first performed an fMRI classifier training experiment on day 1 (Fig. 1B) during which the US^+ and US^- were presented.

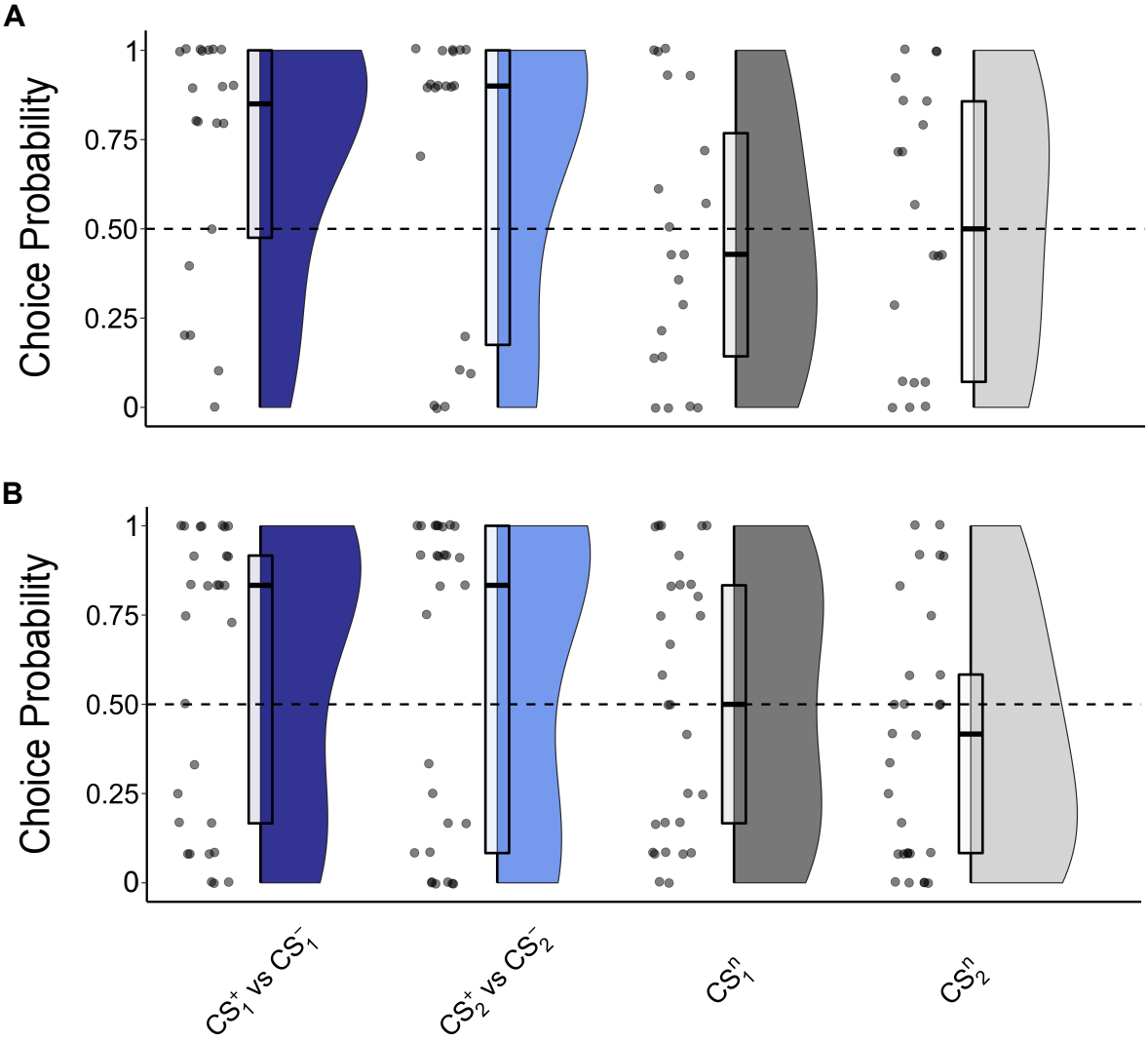

Figure 2. Behavioral results separated for both studies.

Results as in 1F, but separately for the behavioral (A, *N* = 20) and fMRI study (B, *N* = 29). Raincloud plots showing density of choice probability. Box plot center lines represent (pre-averaged) sample medians and box bottom/top edges show 25th/75th percentile of the (pre-averaged) data, respectively.

A multivariate pattern classifier (linear support vector machine, C-SVM) was trained on the fMRI data from this session. On day 2, during SOC, we used the weights of the classifier trained on gustatory neural patterns to predict the class label of the visual CS (Fig. 1D) that had been paired with the US during FOC (Fig. 1C, see Methods and Fig. 3A for schematic of the classification approach). In other words, we used data from one sensory modality, assessed during a first day to train a classification model and tested the model's generalizability to unseen data from another sensory modality on a second day. We found

evidence for reinstatement of US patterns in a region in the left lateral orbitofrontal cortex (lOFC). In this region, it was possible to predict the class labels of neural CS patterns based on US pattern information obtained during classifier training on the previous day. Classification with a 3-mm searchlight revealed a small-volume corrected cluster of above-chance level (0.5) classification accuracy (extracted cluster mean = 0.56, *SD* = 0.07) in the left lateral OFC (lOFC, Fig. 3B, peak voxel at MNI [x = –21, y = 30, z = –17], z = 2.26, P = 0.012, random-effect cluster corrected (Stelzer et al., 2013), 50,000 iterations, one-tailed). The location of this lOFC cluster is consistent with this region's well-documented role in gustatory processing, particularly in representing motivational (Small et al., 1999; Rolls, 2000, 2006) aspects of gustatory sensation and taste memory (Kobayashi et al., 2004). To ensure that our results are not dependent on this particular choice of ROI, we repeated the same analysis using two different, independent ROIs. The first was an anatomical mask of lateral orbitofrontal cortex, the second was obtained from an independent gustatory mapping study by Benz and colleagues (K. Benz, personal communication, 12/2019). We found similar results in the left lOFC anatomical ROI (peak voxel at MNI [x = –21, y = 30, z = –17], z = 1.96, P = .024, corrected, one-tailed) and in the mask from Benz and colleagues (peak voxel at MNI [x = –21, y = 30, z = –17], z = 1.84, P = .033, corrected, one-tailed).

When we split participants into a high- and low-bias group, depending on their preference for the CS_2^+, we observed that significant classification of CS labels in lOFC was possible in the high bias group (Z = 3.43, P = .006, $U3_1$ = .88, one-sample Wilcoxon signed-rank test, two-tailed), but not in the low bias group (Z = 1.44, P = .151, $U3_1$ = .58, one-sample Wilcoxon signed-rank test, two-tailed, Fig. 3C). However, there was no significant difference in classification accuracies in lOFC between the high bias and low bias group (t_{27} = 0.47, P = .320, $U3$ = .50, two-sample t-test, one-tailed; please note that due to the unbalanced number of subjects in both bias groups it was not possible to perform a non-parametric test).

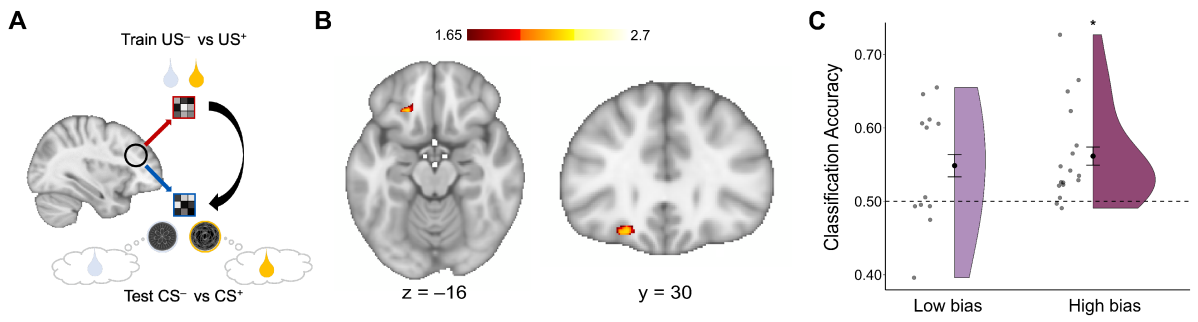

Figure 3. Reinstatement of US representations during second-order conditioning. A) Analysis approach: For cross-session, cross-modality classification, a multivariate classifier was trained on the spatial activation patterns (*t* maps) of US^+ versus US^- (obtained from the classifier training session) and tested on CS_2^+/CS_1^+ versus CS_2^-/CS_1^- during SOC. CS_2^n/CS_1^n related activations were subtracted to control for general visual effects. B) Classification accuracy exceeded chance level (0.5) in a small-volume corrected cluster in the left lateral orbitofrontal cortex (lOFC), using random-effect cluster-statistics (Stelzer et al., 2013). C) Average classification accuracy in the lOFC cluster (extracted cluster mean = 0.56, *SD* = 0.07) was significantly above chance level in the high bias group of participants showing higher than chance preference for CS_2^+, but not in the low bias group. However, there was no significant difference in classification accuracies in lOFC between the high bias and low bias group. Color bar represents *Z*-values. Black dots indicate sample means and error bars represent standard errors of the means of the data, respectively.

Interaction between lOFC, amygdala, and medial OFC during second-order conditioning

To form an associative link between CS_2 and US, the reinstated US patterns need to be projected from their cortical storage site to regions like amygdala and hippocampus, allowing for convergence of US and CS_2 information. We investigated BOLD signal covariation of the cluster in the left lOFC with the whole brain during SOC using two separate psychophysiological interaction (PPI) analyses. In the first PPI, we investigated general covariation differences in response to CS^- and CS^+ relative to CS^n, reasoning that in the former, but not in the latter, reinstated US representations need to be linked with the CS. We found that covariation of BOLD signal in the left lOFC with a cluster in the left hippocampus, extending to amygdala and medial temporal lobe (Fig. 4A, peak voxel at MNI [x = –38, y = –11, z = –24], Z = 3.75, *P* = .003, whole-brain corrected) and a cluster in the right inferior temporal gyrus,

extending to the right hippocampus (peak voxel at MNI [x = 40, y = –32, z = –20], Z = 3.55, *P* = 0.007, whole-brain corrected) was higher in CS^- and CS^+ compared to CS^n trials. Despite the fact that we used an approach with high statistical sensitivity for group-level cluster-based inference (FSL's FLAME1+2 (Beckmann et al., 2003)), a robust estimation technique that yields low family-wise errors rates even at liberal activation thresholds ($Z > 2.3$, corresponding to $p < 0.05$) (Eklund et al., 2016), we would like to note that the aforementioned result did not survive whole-brain correction at more conservative thresholds (e.g. $Z > 2.6$). Furthermore, in the same PPI analysis, we found a positive correlation between second-order choice preference and functional covariation of the left lOFC with a region in the right and left lateral prefrontal cortex (Fig. 5, right peak voxel at MNI [x = 49, y = 41, z = 7], Z = 3.80, *P* < 0.001, whole-brain corrected; left peak voxel at MNI [x = –45, y = 46, z = –4], Z = 3.93, *P* = 0.010, whole-brain corrected). The more participants preferred CS_2^+ (versus CS_2^-), the stronger these regions' BOLD signal covaried during SOC. Some studies hint at complex interactions between OFC and amygdala that differ between appetitive and aversive stimuli (Morrison et al., 2011). Therefore, we next asked whether there were any specific differences between CS^- and CS^+ trials in lOFC BOLD signal covariation with other regions. We found that covariation of the BOLD signal in the left lOFC was higher in CS^+ compared to CS^- trials in a cluster located in the medial OFC, extending to subgenual anterior cingulate cortex (Fig. 4B, peak voxel at MNI [x = 10, y = 50, z = –1], Z = 3.90, *P* < 0.001, whole-brain corrected) and a cluster in the left anterior insula, extending to left caudo-lateral OFC and temporal pole (peak voxel at MNI [x = –51, y = 18, z = –11], Z = 3.33, *P* = 0.004, whole-brain corrected). Given both the difficulties in inferring directionality from fMRI data and the reciprocal nature of connections between lOFC and both amygdala and medial OFC, a directionality of our PPI results cannot be determined.

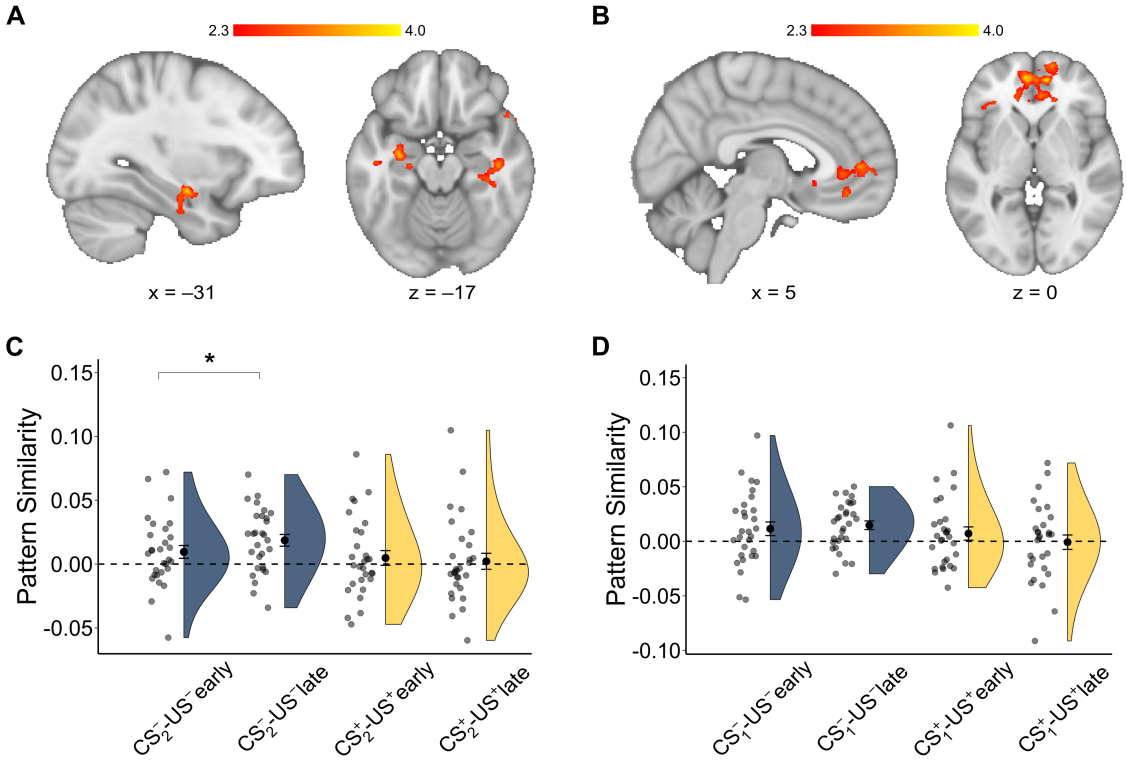

Figure 4. Psychophysiological interaction analyses and neural pattern similarity results.

A) BOLD covariation was higher in CS^- and CS^+ trials than in CS^n trials between the left lOFC and a cluster in the anterior hippocampus, extending to (basolateral) amygdala and medial temporal lobe and a cluster in the right inferior temporal gyrus, extending to the right hippocampus. B) Covariation of BOLD signal in the left lOFC was higher in CS^+ trials compared to CS^- trials in a cluster located in the medial OFC, extending to subgenual anterior cingulate cortex. C, D) Template-based neural pattern similarity between US patterns from the classifier training experiment and CS_2 (C) and CS_1 (D) patterns during SOC, separately estimated for early (first 25 trials) and late (last 25 trials) of SOC in a bilateral amygdala ROI. C) CS_2^- and US^- patterns became more similar from early to late trials. However, there was no evidence for a difference between early and late trial similarity for CS_2^+ and US^+. D) There was no evidence for change in similarity for CS_1^--US^- or CS_1^+-US^+ neural pattern similarity. Black dots indicate sample means and error bars represent standard errors of the means of the data, respectively. Color bars represent *Z*-values.

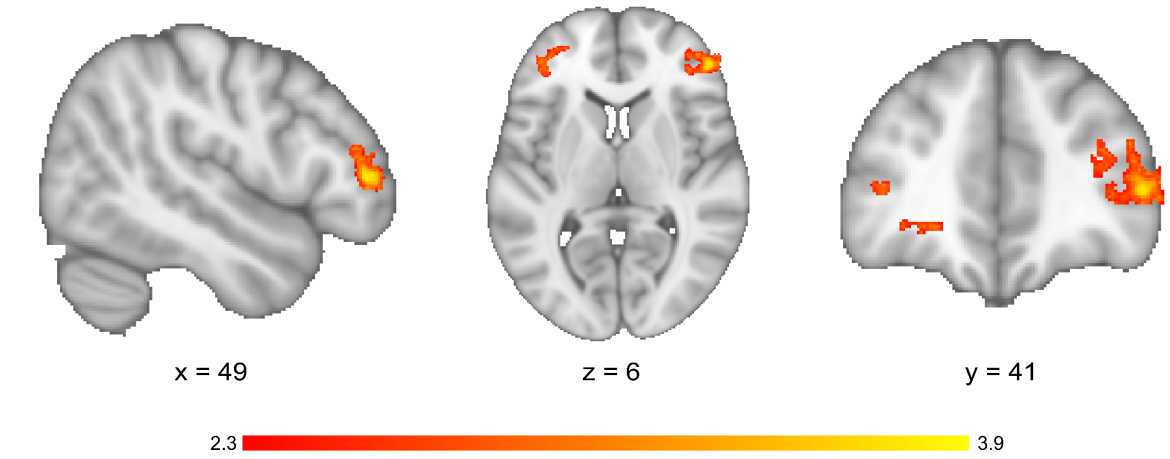

Figure 5. Psychophysiological interaction analyses: Association with second-order choice preferences.

A positive correlation was observed between second-order choice preferences (CS_2^+ versus CS_2^-) and functional covariation between the left lOFC and a region in the right and left lateral prefrontal cortex. The more participants preferred CS_2^+ (versus CS_2^-), the higher these regions' activation covaried during second-order conditioning. Color bar represents *Z*-values.

Plasticity of association between second-order CS and US in the amygdala

We reasoned that if the amygdala uses the reinstated cortical outcome pattern in lOFC to acquire an association between CS_2 and the respective US, one would expect similarity between the neural patterns evoked by CS_2 and US, respectively. This similarity should increase over the course of second-order conditioning, as the association is being acquired. Importantly, during the classifier training experiment, there was evidence for US representations in the amygdala. We found differential neural patterns in response to US^- and US^+ in the amygdala (among other regions) using an exploratory leave-one-run-out cross-validated classification analysis on the neural pattern recorded during the classifier training experiment (Fig. 6). Using a least-squares separate (LS-S) approach (Mumford et al., 2012) to deconvolve single-trial estimates, we first computed overall neural pattern similarity (Kriegeskorte et al., 2008) between the pattern evoked by CS_2 (during SOC) and their respective US (during classifier training) in the bilateral amygdala. There was significant

pattern similarity between CS_2^- and US^- (t_{28} = 3.38, P = 0.002, $U3_1$ = 0.79; but not between CS_2^+ and US^+, t_{28} = 0.74, P = 0.464, $U3_1$= 0.55). We reason that this could be due to differential motivational aspects of the gustatory outcomes we used. The US^- consisted of an aversively tasting quinine solution, which has been shown to produce innate avoidance responses that are not thought to be generated by learning (Yiannakas and Rosenblum, 2017). In contrast, US^+ was orange juice, a compound stimulus that consists of many taste features (e.g. sour and fruity components), next to sweet sensation, which also produces innate responses (Yiannakas and Rosenblum, 2017). Presumably, this heterogeneity of taste facets in US^+ had induced more variability in taste responses in our participants. Additionally, it appears likely that in a society offering sugary and highly palatable foods and drinks in abundance, US^+ (an orange juice, most likely a very familiar taste to most of our participants) might not have been perceived as rewarding, or novel enough to represent a motivationally relevant and salient event for our participants. It might well be that participants did not have experience with the aversive taste of quinine, rendering it a novel and salient gustatory sensation, presumably resulting in only the US^- being considered behaviorally and motivationally relevant. Thus, it is possible that the observed preference for CS_1^+ and CS_2^+ was indeed due to an aversion against CS_1^- and CS_2^-. If the observed neural pattern similarity between CS_2 and US indeed reflects the formation of an associative link during second-order learning, one would expect the observed similarity to increase from early to late stages of learning, as the association is being acquired and the CS_2 comes to predict the US. We therefore compared our measure of neural pattern similarity between early and late trials of SOC. As expected, neural pattern similarity between CS_2^- and US^- in the bilateral amygdala ROI increased from early to late trials of SOC (t_{28} = 1.88, P = 0.035, Cohen's d = 0.35, paired-samples t-test, one-tailed, Fig. 4C). This change in similarity was not observed for the first-order CS_1^+-US^+ or CS_1^--US^- pattern similarity (Fig. 4D), nor for second-order CS_2^+-US^+ similarity (all P > .310, paired-samples t-tests, one-tailed, Fig. 4C).

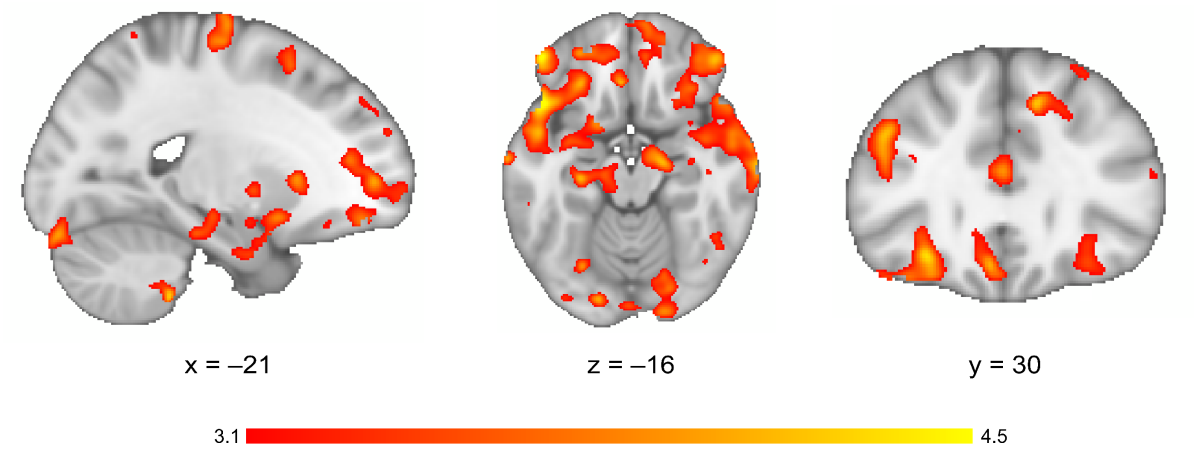

Figure 6. US$^+$ versus US$^-$ classification.

Group average (*N* = 29) cross-validated predictive accuracy for US$^+$ versus US$^-$ activation patterns during the classifier training experiment. As an exploratory analysis, we used multivariate searchlight classification (3-mm searchlight spheres) to distinguish between the spatial activation patterns (*t* maps) of US$^+$ versus US$^-$ across the whole brain, resulting in one whole-brain map of classification accuracies per participant. This classification was performed using a 5-fold cross-validation scheme. Data was averaged across participants and smoothed with a Gaussian kernel with 5 mm FWHM. Please note that due to the exploratory nature and illustrative purpose of this analysis, no multiple comparisons correction using random-effects cluster-statistics was performed. Color bar represents uncorrected *Z*-values.

Discussion

Using a second-order conditioning paradigm, we provided evidence for associative transfer of value during higher-order conditioning. Decisions were biased by values indirectly acquired by second-order learning. Participants were more likely to select directly and indirectly appetitively paired stimuli over aversively paired stimuli, closely resembling rodent studies describing instrumental behavior guided by second-order conditioning (Sharpe et al., 2017; Maes et al., 2020). Notably, choice biases for second-order conditioned stimuli in the present study emerged in the absence of explicit knowledge of the underlying higher-order associative structure. This suggests that humans, similar to rodents, implicitly acquire preferences through higher-order transfer learning mechanisms – extending previous studies promoting acquisition of explicit associative relationships between stimuli (Jara et al., 2006; Pauli et al., 2019; Wang

et al., 2020). The present study thus demonstrates that human value-based decision making is affected by motivational value implicitly conferred via second-order conditioning. Our study is – to the best of our knowledge – the only report so far demonstrating that human binary decision making is governed by motivational value transfer via second-order conditioning. Although there is a rich literature on second-order conditioning, direct evidence for this phenomenon in humans using similar procedures as in previous animal work was lacking. Our study enables a closer comparison between humans and other species during higher-order learning. Moreover, even animal studies, albeit well-covering Pavlovian settings (Gewirtz and Davis, 2000; Sharpe et al., 2017), have thus far not reported effects of second-order conditioning on binary choice behavior.

Thus far, most studies investigating higher-order learning effects in humans have used sensory preconditioning procedures (Wimmer and Shohamy, 2012; Kurth-Nelson et al., 2015; Wang et al., 2020). Theoretical accounts and empirical findings suggest that the value structure acquired during sensory preconditioning and second-order conditioning – despite the close conceptual links between paradigms – differs fundamentally. In sensory preconditioning, a stimulus-stimulus association is acquired first (preconditioning phase), before one stimulus is paired with an outcome (conditioning phase). It has been found that preconditioned stimuli do not directly acquire value, as they do not serve as conditioned reinforcers (Sharpe et al., 2017). Instead, preconditioned stimuli reactivate both conditioned stimuli and indirectly associated outcome representations at preference assessment (Barron et al., 2020; Wang et al., 2020), suggesting value inference based on associative chaining. Contrarily, during second-order conditioning, second-order CS directly acquire value, allowing them to act as conditioned reinforcers (Sharpe et al., 2017). These findings indicate that associative transfer of motivational value from outcomes to higher-order, indirectly paired CS are observed in second-order conditioning, but not in sensory preconditioning.

We found reinstatement of neural representations of gustatory outcomes by directly paired visual first-order CS. This reinstatement occurred in a region in the rostrolateral OFC, which has previously been implicated in representing stimulus-outcome associations (Klein-

Flügge et al., 2013; Jocham et al., 2016; Luettgau et al., 2020) and in correctly assigning credit for a reward to the causal stimulus choice (Walton et al., 2010; Jocham et al., 2016). It is also part of the network most consistently involved in taste processing (Neurosynth, Yarkoni et al., 2011) and plays a well-documented role in representing motivational aspects of gustatory sensation (Small et al., 1999; Rolls, 2000, 2006) and taste memory (Kobayashi et al., 2004). Importantly, we had trained the classifier on gustatory US prior to pairing them with first-order CS (on a separate day). Thus, decoding of the visual CS during second-order learning cannot be spuriously driven by visual responses elicited by the US or the visual swallowing cue during classifier training. Despite the fact that the classifier was tested on the entire activation pattern elicited by the CS_1-CS_2-pairs, US reinstatement during second-order conditioning is most likely attributable to the respective CS_1. This is due to the fact that, despite the close temporal proximity with CS_2, only CS_1, but not CS_2, had been directly paired with the outcome and should thus elicit a US representation (Wagner, 1981). Since we had optimized our design for behavioral second-order learning effects by introducing only small temporal offsets between first- and second-order CS, methods with higher temporal resolution as fMRI would be required to dissociate the specific responses to CS_1, and CS_2.

OFC clearly does not act in isolation. The OFC region in which we observed reinstatement of outcome representations displayed increased task-related BOLD signal covariation with amygdala, anterior hippocampus, and medial OFC during second-order learning. Neurons in OFC and amygdala show complex, bi-directional interactions during acquisition and reversal of outcome-predictive associations (Morrison et al., 2011). Functional disconnection of OFC and amygdala using asymmetric lesions produces deficits in flexibly adjusting behavior to changes in stimulus value (Baxter et al., 2000; Fiuzat et al., 2017). We also observed that representations of visual second-order CS in amygdala became more similar to gustatory US representations from early to late phases of second-order conditioning. This indicates development of an associative link between CS_2 and US, consistent with the finding that both amygdala and hippocampal lesions impair second-order learning (Gewirtz and Davis, 1997; Gilboa et al., 2014).

Similar to the present results, two previous fMRI studies in humans used sequential Pavlovian conditioning paradigms to investigate higher-order learning. Whereas Seymour and colleagues (Seymour et al., 2004) find that human learning about sequentially presented pain-predictive stimuli relies on the formation of stimulus-stimulus associations and follows temporal difference learning algorithms, putatively implemented in the striatum, Pauli and colleagues (Pauli et al., 2019) provide evidence for model-based representation of stimulus-stimulus associations in the lateral OFC. However, in both paradigms, two CS and a US are presented in close temporal proximity within the same trial. These previous studies differ from the present approach in two important ways. Firstly, unlike second-order conditioning, both paradigms do not require any reinstatement of US representations, nor any transfer of value, but rather impose different temporal offsets between CS and US, as indicated by temporal difference models used to explain the data (Seymour et al., 2004). This sharply contrasts with second-order conditioning, where CS_2 is presented in a separate block that is entirely devoid of US presentations. Secondly, in both studies, it is difficult to dissociate the activation patterns related to the proximal CS (Pauli et al., 2019) or Cue B/D (Seymour et al., 2004) (CS_1 in second-order conditioning), CS-related anticipatory pre-activation of US representations and the neural activation related to the US presentation. In contrast, here we trained the classifier on the (gustatory) US on a separate day and then tested on the (visual) CS presented during the second-order learning phase.

Our study presents a neural mechanism for associative transfer learning in second-order conditioning, which thus far has remained unclear. At least four potential mechanisms have been proposed (Rizley and Rescorla, 1972; Barnet et al., 1991; Gewirtz and Davis, 2000). Three of these suggest that CS_2 could become associated with a CR using (i) the associative link between stimulus representations of CS_2 and CS_1, (ii) direct pairing of the CS_1-evoked CR with CS_2, or (iii) because CS_1 reactivates US representations which then evoke a CR that becomes paired with CS_2. Previous studies clearly suggest that neither of these three hypotheses can account for second-order learning effects (Rizley and Rescorla, 1972; Barnet et al., 1991). It has been shown that CRs towards CS_2 are unaffected by CS_1 extinction after

second-order conditioning (Rizley and Rescorla, 1972; Barnet et al., 1991). Additionally, CS_2 and CS_1 tend to produce qualitatively different CRs (Gewirtz and Davis, 2000) and the magnitudes of CRs appear largely uncorrelated (Barnet et al., 1991). Together, these previous findings make it highly implausible that CS_2–CS_1 associations are necessary for the expression of CS2-related CRs, or that CS_2 could be associated with CRs elicited by CS_1. Here, we provide evidence for a fourth possibility (Gewirtz and Davis, 2000; Parkes and Westbrook, 2011): that CS_2 is directly paired with a neural representation of the US, or with the motivational state conveyed by the US. Our results suggest that, during second-order conditioning, outcome representations are reinstated in the lateral OFC. Information of reinstated outcome representations could be communicated between lOFC and amygdala/anterior hippocampus for associative linking between neutral stimuli and outcomes. It should be noted that the present design does not allow us to dissociate whether the reinstated US representations detected by the classification algorithm pertain to the value, intensity or sensory features of the US – or a combination of these features. However, the question which of these features was reinstated by CS_1 and contributed to the associative transfer of value to CS_2 is beyond the scope of the present study.

How the reinstatement of cortical US patterns found in our study relates to the observation in rats that midbrain dopamine neurons acquire temporal difference error signals in response to CS_2 (Maes et al., 2020) presents an important question for future studies. Furthermore, it would be of great interest to elucidate the directionality and exact content of information flow between lOFC and amygdala/anterior hippocampus, and whether this transfer of information is supported by phase coherence in theta oscillations (Benchenane et al., 2010; Young and Shapiro, 2011; Knudsen and Wallis, 2020).

Taken together, our data support the idea that during second-order conditioning, second-order CS and representations of outcomes – events that had never been explicitly paired during the individual's learning history – can be linked by exploiting the relational structure of events. The present study enables a closer comparison between humans and other species during higher-order learning. In conclusion, our results suggest a neural

mechanism by which outcome representations can be propagated to stimuli that are never experienced in contiguity with reinforcement, allowing for credit assignment in real-world learning scenarios with infrequent direct encounters with rewards or punishments.

Conflict of interests: Authors declare no conflict of interests.

Acknowledgments

The authors thank all volunteers who participated in this study. The authors would like to thank Halla Mulla-Osman, Stefanie Linnhoff, Leonie Oevel and Denise Scheermann for their invaluable support during data acquisition. Additionally, we thank Gunnar and Christian Lüttgau for electrical engineering support during construction of the gustometer, Karsta Benz for helpful discussions during the set-up of the study and Denise Kramer for production of the gustatory stimuli. We thank the Center for Magnetic Resonance Research of the University of Minnesota for providing the Multiband accelerated fMRI sequence. Computational infrastructure and support were provided by the Centre for Information and Media Technology at Heinrich Heine University Düsseldorf. **Funding:** This work was funded by the federal state of Saxony-Anhalt and the „European Regional Development Fund“ (ERDF 2014-2020), Vorhaben: Center for Behavioral Brain Sciences (CBBS), FKZ: ZS/2016/04/78113; **Author contributions:** LL designed the study and conceptualized research, acquired the data, analyzed the data, drafted the manuscript, read and edited versions of the manuscript and approved the final version of the manuscript. EP analyzed the data, read and edited versions of the manuscript and approved the final version of the manuscript. CT set up the MRI acquisition protocol, read and edited versions of the manuscript and approved the final version of the manuscript. GJ designed the study and conceptualized research, analyzed the data, read and edited versions of the manuscript and approved the final version of the manuscript.

References

Abdulrahman H, Henson RN (2016) Effect of trial-to-trial variability on optimal event-related fMRI design: Implications for Beta-series correlation and multi-voxel pattern analysis. Neuroimage 125:756–766 Available at: http://dx.doi.org/10.1016/j.neuroimage.2015.11.009.

Allen M, Poggiali D, Whitaker K, Marshall TR, Kievit RA (2019) Raincloud plots: A multi-platform tool for robust data visualization [version 1; peer review: 2 approved]. Wellcome Open Res 4:1–41.

Andersson JL., Jenkinson M, Smith S (2007a) Non-linear registration aka spatial normalisation. FMRIB Tech Rep TRO7JA2:22 Available at: http://fmrib.medsci.ox.ac.uk/analysis/techrep/tr07ja2/tr07ja2.pdf.

Andersson JL., Jenkinson M, Smith SM (2007b) Non-linear optimisation. FMRIB Tech Rep TRO7JA1.

Barnet RC, Arnold HM, Miller RR (1991) Simultaneous conditioning demonstrated in second-order conditioning: Evidence for similar associative structure in forward and simultaneous conditioning. Learn Motiv 22:253–268.

Barron HC, Reeve HM, Koolschijn RS, Perestenko P V., Shpektor A, Nili H, Rothaermel R, Campo-Urriza N, O'Reilly JX, Bannerman DM, Behrens TEJ, Dupret D (2020) Neuronal Computation Underlying Inferential Reasoning in Humans and Mice. Cell 183:228-243.e21.

Baxter MG, Parker A, Lindner CCC, Izquierdo AD, Murray EA (2000) Control of response selection by reinforcer value requires interaction of amygdala and orbital prefrontal cortex. J Neurosci 20:4311–4319.

Beckmann CF, Jenkinson M, Smith SM (2003) General multilevel linear modeling for group analysis in FMRI. Neuroimage 20:1052–1063.

Benchenane K, Peyrache A, Khamassi M, Tierney PL, Gioanni Y, Battaglia FP, Wiener SI (2010) Coherent Theta Oscillations and Reorganization of Spike Timing in the Hippocampal- Prefrontal Network upon Learning. Neuron 66:921–936 Available at: http://dx.doi.org/10.1016/j.neuron.2010.05.013.

Boorman ED, Rajendran VG, O'Reilly JX, Behrens TE (2016) Two Anatomically and Computationally Distinct Learning Signals Predict Changes to Stimulus-Outcome Associations in Hippocampus. Neuron 89:1343–1354 Available at: http://dx.doi.org/10.1016/j.neuron.2016.02.014.

Brainard DH (1997) The Psychophysics Toolbox. Spat Vis 10:433–436.

Development Team S (2020) RStan: the R interface to Stan. Available at: http://mc-stan.org/.

Eklund A, Nichols TE, Knutsson H (2016) Cluster failure: Why fMRI inferences for spatial extent have inflated false-positive rates. Proc Natl Acad Sci 113:7900–7905 Available at: http://www.pnas.org/lookup/doi/10.1073/pnas.1602413113 [Accessed August 1, 2016].

Fiuzat EC, Rhodes SEV, Murray EA (2017) The role of orbitofrontal-amygdala interactions in updating action-outcome valuations in macaques. J Neurosci 37:2463–2470.

Gewirtz JC, Davis M (1997) Second-order fear conditioning prevented by blocking NMDA receptors in amygdala. Nature 388:471–474.

Gewirtz JC, Davis M (2000) Using Pavlovian higher-order conditioning paradigms to investigate the neural substrates of emotional learning and memory. Learn Mem 7:257–266.

Gilboa A, Sekeres M, Moscovitch M, Winocur G (2014) Higher-order conditioning is impaired by hippocampal lesions. Curr Biol 24:2202–2207.

Griffanti L, Douaud G, Bijsterbosch J, Evangelisti S, Alfaro-Almagro F, Glasser MF, Duff EP, Fitzgibbon S, Westphal R, Carone D, Beckmann CF, Smith SM (2017) Hand classification of fMRI ICA noise components. Neuroimage 154:188–205 Available at: https://www.sciencedirect.com/science/article/pii/S1053811916307583?via%3Dihub [Accessed June 15, 2019].

Hatfield T, Han JS, Conley M, Gallagher M, Holland P (1996) Neurotoxic lesions of basolateral, but not central, amygdala interfere with pavlovian second-order conditioning and reinforcer devaluation effects. J Neurosci 16:5256–5265.

Hentschke H (2020) hhentschke/measures-of-effect-size-toolbox (https://www.github.com/hhentschke/measures-of-effect-size-toolbox), GitHub. Retrieved January 10, 2020.

Jara E, Vila J, Maldonado A (2006) Second-order conditioning of human causal learning. Learn Motiv 37:230–246.

Jenkinson M (2003) Fast, automated,N-dimensional phase-unwrapping algorithm. Magn Reson Med 49:193–197 Available at: http://doi.wiley.com/10.1002/mrm.10354 [Accessed October 9, 2019].

Jenkinson M, Bannister P, Brady M, Smith S (2002) Improved Optimization for the Robust

and Accurate Linear Registration and Motion Correction of Brain Images. Neuroimage 17:825–841 Available at: https://www.sciencedirect.com/science/article/pii/S1053811902911328?via%3Dihub [Accessed October 9, 2019].

Jenkinson M, Beckmann CF, Behrens TEJ, Woolrich MW, Smith SM (2012) FSL. Neuroimage 62:782–790 Available at: https://www.sciencedirect.com/science/article/pii/S1053811911010603?via%3Dihub [Accessed June 15, 2019].

Jocham G, Brodersen KHH, Constantinescu AOO, Kahn MCC, Ianni AM, Walton MEE, Rushworth MFFS, Behrens TEEJ (2016) Reward-Guided Learning with and without Causal Attribution. Neuron 90:177–190 Available at: http://www.ncbi.nlm.nih.gov/pubmed/26971947 [Accessed June 17, 2019].

Klein-Flügge MC, Barron HC, Brodersen KH, Dolan RJ, Behrens TEJ (2013) Segregated Encoding of Reward-Identity and Stimulus-Reward Associations in Human Orbitofrontal Cortex. J Neurosci 33:3202–3211 Available at: http://www.jneurosci.org/cgi/doi/10.1523/JNEUROSCI.2532-12.2013.

Knudsen EB, Wallis JD (2020) Closed-Loop Theta Stimulation in the Orbitofrontal Cortex Prevents Reward-Based Learning. Neuron 106:537-547.e4 Available at: https://doi.org/10.1016/j.neuron.2020.02.003.

Kobayashi M, Takeda M, Hattori N, Fukunaga M, Sasabe T, Inoue N, Nagai Y, Sawada T, Sadato N, Watanabe Y (2004) Functional imaging of gustatory perception and imagery: “Top-down” processing of gustatory signals. Neuroimage 23:1271–1282.

Kriegeskorte N, Goebel R, Bandettini P (2006) Information-based functional brain mapping. Proc Natl Acad Sci U S A 103:3863–3868.

Kriegeskorte N, Mur M, Bandettini P (2008) Representational similarity analysis – connecting the branches of systems neuroscience. Front Syst Neurosci 2:1–28.

Kurth-Nelson Z, Barnes G, Sejdinovic D, Dolan R, Dayan P (2015) Temporal structure in associative retrieval. Elife 4:1–18.

Luettgau L, Tempelmann C, Kaiser LF, Jocham G (2020) Decisions bias future choices by modifying hippocampal associative memories. Nat Commun 11:3318 Available at: https://www.biorxiv.org/content/10.1101/802462v1.

Maes EJP, Sharpe MJ, Usypchuk AA, Lozzi M, Chang CY, Gardner MPH, Schoenbaum G, Iordanova MD (2020) Causal evidence supporting the proposal that dopamine

transients function as temporal difference prediction errors. Nat Neurosci 23:176–178 Available at: http://dx.doi.org/10.1038/s41593-019-0574-1.

Makowski D, Ben-Schachar M, Lüdecke D (2019) bayestestR: Describing Effects and their Uncertainty, Existence and Significance within the Bayesian Framework. J Open Source Softw 4:1541.

Mcdannald MA, Setlow B, Holland PC (2013) Effects of ventral striatal lesions on first- and second-order appetitive conditioning. Eur J Neurosci 38:2589–2599.

McElreath R (2020) rethinking: Statstical rethinking book package.

Miranda MI (2012) Taste and odor recognition memory: The emotional flavor of life. Rev Neurosci 23:481–499.

Morrison SE, Saez A, Lau B, Salzman CD (2011) Different Time Courses for Learning-Related Changes in Amygdala and Orbitofrontal Cortex. Neuron 71:1127–1140 Available at: http://dx.doi.org/10.1016/j.neuron.2011.07.016.

Mumford JA, Turner BO, Ashby FG, Poldrack RA (2012) Deconvolving BOLD activation in event-related designs for multivoxel pattern classification analyses. Neuroimage 59:2636–2643 Available at: http://dx.doi.org/10.1016/j.neuroimage.2011.08.076.

Oosterhof NN, Connolly AC, Haxby J V, Rosa MJ (2016) CoSMoMVPA : Multi-Modal Multivariate Pattern Analysis of Neuroimaging Data in Matlab / GNU Octave. 10:1–27.

Parkes SL, Westbrook RF (2011) Role of the basolateral amygdala and NMDA receptors in higher-order conditioned fear. Rev Neurosci 22:317–333.

Pauli WM, Gentile G, Collette S, Tyszka JM, O'Doherty JP (2019) Evidence for model-based encoding of Pavlovian contingencies in the human brain. Nat Commun 10:1099 Available at: https://europepmc.org/articles/PMC6405831.

Pavlov IP (1927) Conditioned Reflexes. London: Oxford University Press. Available at: https://books.google.de/books?id=XbOjAQAAQBAJ.

Rizley RC, Rescorla RA (1972) Associations in second-order conditioning and sensory preconditioning. J Comp Physiol Psychol 81:1–11.

Rolls ET (2000) The Orbitofrontal Cortex and Reward. Cereb Cortex 10:284–294.

Rolls ET (2006) Brain mechanisms underlying flavour and appetite. Philos Trans R Soc B Biol Sci 361:1123–1136.

RStudioTeam (2019) RStudio: Integrated Development for R. Available at: http://www.rstudio.com/.

Setlow B, Gallagher M, Holland PC (2002) The basolateral complex of the amygdala is necessary for acquisition but not expression of CS motivational value in appetitive Pavlovian second-order conditioning. Eur J Neurosci 15:1841–1853.

Seymour B, O'Doherty JP, Dayan P, Koltzenburg M, Jones AK, Dolan RJ, Friston KJ, Frackowiak RS (2004) Temporal difference models describe higher-order learning in humans. Nature 429:664–667.

Sharpe MJ, Batchelor HM, Schoenbaum G (2017) Preconditioned cues have no value. Elife 6.

Small DM, Zald DH, Jones-Gotman M, Zatorre RJ, Pardo J V., Frey S, Petrides M (1999) Human cortical gustatory areas: A review of functional neuroimaging data. Neuroreport 10:7–14.

Stelzer J, Chen Y, Turner R (2013) Statistical inference and multiple testing correction in classification-based multi-voxel pattern analysis (MVPA): Random permutations and cluster size control. Neuroimage 65:69–82 Available at: https://www.sciencedirect.com/science/article/abs/pii/S1053811912009810 [Accessed March 17, 2020].

Stokes M, Thompson R, Cusack R, Duncan J (2009) Top-down activation of shape-specific population codes in visual cortex during mental imagery. J Neurosci 29:1565–1572.

Tamaoka K, Makioka S, Sanders S, Verdonschot RG (2017) www.kanjidatabase.com: a new interactive online database for psychological and linguistic research on Japanese kanji and their compound words. Psychol Res 81:696–708 Available at: https://doi.org/10.1007/s00426-016-0764-3.

Tonegawa S, Morrissey MD, Kitamura T (2018) The role of engram cells in the systems consolidation of memory. Nat Rev Neurosci 19:485–498 Available at: http://dx.doi.org/10.1038/s41583-018-0031-2.

Wagner AR (1981) SOP : A model of automatic processing in animal behavior. In: Information Processing in Animals: Conditioned Inhibition, pp 5–24.

Walton ME, Behrens TEJ, Buckley MJ, Rudebeck PH, Rushworth MFS (2010) Separable Learning Systems in the Macaque Brain and the Role of Orbitofrontal Cortex in Contingent Learning. Neuron 65:927–939.

Wang F, Schoenbaum G, Kahnt T (2020) Interactions between human orbitofrontal cortex and hippocampus support model-based inference. PLoS Biol 18:1–24 Available at: http://dx.doi.org/10.1371/journal.pbio.3000578.

Wimber M, Alink A, Charest I, Kriegeskorte N, Anderson MC (2015) Retrieval induces adaptive forgetting of competing memories via cortical pattern suppression. Nat Neurosci 18:582–589 Available at: http://dx.doi.org/10.1038/nn.3973.

Wimmer GE, Shohamy D (2012) Preference by Association: How Memory Mechanisms in the Hippocampus Bias Decisions. Science 338:270–273.

Woolrich MW, Ripley BD, Brady M, Smith SM (2001) Temporal Autocorrelation in Univariate Linear Modeling of FMRI Data. Neuroimage 14:1370–1386 Available at: https://www.sciencedirect.com/science/article/pii/S1053811901909310?via%3Dihub [Accessed October 9, 2019].

Yarkoni T, Poldrack RA, Nichols TE, Van Essen DC, Wager TD (2011) Large-scale automated synthesis of human functional neuroimaging data. Nat Methods 8:665–670.

Yiannakas A, Rosenblum K (2017) The insula and taste learning. Front Mol Neurosci 10:1–24.

Young JJ, Shapiro ML (2011) Dynamic coding of goal-directed paths by orbital prefrontal cortex. J Neurosci 31:5989–6000.